Power Spectral Density of Unevenly Sampled Data by Least-Square Analysis: Performance and Application to Heart Rate Signals

Pablo Laguna,* *Member, IEEE*, George B. Moody, *Associate Member, IEEE*, and Roger G. Mark, *Senior Member, IEEE*

***Abstract*—This work studies the frequency behavior of a least-square method to estimate the power spectral density of unevenly sampled signals. When the uneven sampling can be modeled as uniform sampling plus a stationary random deviation, this spectrum results in a periodic repetition of the original continuous time spectrum at the mean Nyquist frequency, with a low-pass effect affecting upper frequency bands that depends on the sampling dispersion. If the dispersion is small compared with the mean sampling period, the estimation at the base band is unbiased with practically no dispersion. When uneven sampling is modeled by a deterministic sinusoidal variation respect to the uniform sampling the obtained results are in agreement with those obtained for small random deviation. This approximation is usually well satisfied in signals like heart rate (HR) series. The theoretically predicted performance has been tested and corroborated with simulated and real HR signals. The Lomb method has been compared with the classical power spectral density (PSD) estimators that include resampling to get uniform sampling. We have found that the Lomb method avoids the major problem of classical methods: the low-pass effect of the resampling. Also only frequencies up to the mean Nyquist frequency should be considered (lower than 0.5 Hz if the HR is lower than 60 bpm). We conclude that for PSD estimation of unevenly sampled signals the Lomb method is more suitable than fast Fourier transform or autoregressive estimate with linear or cubic interpolation. In extreme situations (low-HR or high-frequency components) the Lomb estimate still introduces high-frequency contamination that suggest further studies of superior performance interpolators. In the case of HR signals we have also marked the convenience of selecting a stationary heart rate period to carry out a heart rate variability analysis.**

***Index Terms*— Heart rate variability (HRV), power spectral density (PSD) estimation of unevenly sampled signals, PSD estimate by least squared analysis.**

I. Introduction

HEART rate variability (HRV) has become an interesting and useful tool for analyzing cardiovascular autonomic control from the surface electrocardiogram (ECG) [1]–[9]. HRV is analyzed from the heart rate (HR) series that is formed by a sequence of values at time instants t_n (cardiac beat occurrence), and whose value at time t_n is a function of the previous R-R interval as measured from the electrocardiographic (ECG) signal. This time series is not evenly sampled since the time occurrence of heartbeats do not follow a perfectly regular pattern.

Estimation and quantification of HRV can be performed using several indexes [8]. However, the power spectral density (PSD) of the HR series seems to be the index that best recovers all the information present in the HR series [8]. The PSD must be estimated from a set of unevenly spaced samples. In [10] it was demonstrated that a bandwidth-limited signal is uniquely determined by its values at a set of recurrent nonuniformly distributed sample points $t = \tau_{pm} = t_p + mN/2W$, where t_p $(p = 1,2,\cdots,N)$ are the N uneven sample point in $N/2W$ s of the signal; and $m = \cdots,-1,0,1,\cdots$. W is the maximum frequency component of the signal expressed in Hz. This situation is the case of HRV analyzes where we have N samples nonuniformly spaced. We can suppose the HRV signal repeated itself (periodic) or extended with zeros to fit the previous theorem and then we get that the samples of HRV only give a unique representation of a signal if we assume this is band-limited to the frequency inverse of the mean heart period (RR interval). This is an important observation that leads to only use PSD estimation up to this frequency and not to 0.5 Hz which is so frequently used in literature. When the HR is lower than 60 beats/min (bpm), care should be taken with the upper limit of the high-frequency band.

Estimation of the PSD of HR series can be done with the analytical expressions derived in [10], but in [11] it was noted that even though this estimate is superior to others it is impractical to realize. Estimation of the PSD of HR series by classical methods cannot be done directly from the time series signal. Instead, it requires resampling to achieve uniform time intervals [12]–[14]. This resampling, required in order to use the well-known methods of PSD estimation of evenly sampled signals, introduces low-pass filtering and possible artifacts in the estimated spectrum. Other sources of errors are the sampling rate of the ECG [15], which can be solved by increasing the sampling rate. Errors in QRS detectors and nonstability in PR intervals will also affect the accurate location of fiducial points for HRV. Nevertheless, in practice, QRS detector marks are the most stable locations. The use of HR or heart period (HP) as the analyzed signal also influences the estimated spectrum; in [16] and [17] it is shown that although both signals give similar estimates, the

Manuscript received May 11, 1995; revised November 6, 1997. This work was supported in part by CICYT under Grants TIC94-0608-01:2 and TIC97-0945-C02-01:2 and in part by CONAI under Grant PIT06/93. The work of P. Laguna was supported in part by the "Instituto Aragones de Fomento (IAF)." *Asterisk indicates corresponding author.*

*P. Laguna is with the Grupo de Tecnologías de las Comunicaciones, Departamento de Ingeniería Electrónica y Comunicaciones, Centro Politécnico Superior, Universidad de Zaragoza, C/María de Luna 3, 50015 Zaragoza, Spain (e-mail: laguna@posta.unizar.es).

G. B. Moody and R. G. Mark are with the Division of Health Sciences and Technology, Harvard–Massachusetts Institute of Technology, Cambridge, MA 02139 USA.

Publisher Item Identifier S 0018-9294(98)02871-7.

HR is more adequate. In addition, when ectopic or noisy beat detection occurs, a broadband noise contamination appears in the spectrum. Elimination of these ectopic or noisy beats and subsequent resampling introduces further alteration of the HR spectrum [18], [19]. Another method to estimate the PSD of HR signals is the autoregressive estimate (AR) [20], [21] which also needs resampling and a selection of the model order, both of which affect the results. Recently, it has been pointed out that AR methods can introduce a large dispersion when applied to HR signals [22]. This problem has been recently overcome [23] by using a PSD estimation method that deals with unevenly sampled data. This method was originally proposed by Lomb [24] and has been used for astronomic time series analysis [25]. Using this method (from now on referred to as the Lomb method) it is not necessary to interpolate noisy or ectopic beat detection, thus, avoiding the spectrum distortion previously mentioned.

The Lomb PSD estimation method is based on the general transform theory [26] which shows that the projection of a signal $x(t)$ onto one element of an orthonormal base $b_i(t)$ is the value "c" that minimizes the mean squared error energy $(e(c))$ defined as the integral, over the definition interval, of the squared differences between $x(t)$ and $c \cdot b_i(t)$. The Lomb method implements this minimization over the unevenly distributed sampled values of $x(t)$ considering that the basis functions are the Fourier kernel $b_i(t) = e^{j2\pi f_i t}$.

In this paper, we present a detailed analysis of the frequency behavior of the Lomb PSD estimation method. We have concentrated on HR series and have found the frequency-limit estimation (half the mean HR) up to which the Lomb PSD estimate is free of aliasing or leakage. Finally, we present some examples with simulated and real HR series that corroborate our previous study and show the utility of the Lomb PSD estimate for HR series analysis. The advantages of this estimate compared with the classical estimates are clearly pointed out in terms of the attenuation of the low-pass effect introduced by resampling.

II. The Lomb Power Spectral Density Estimation Method

The Lomb method for power spectral density estimation is based on the minimization of the squared differences between the projection of the signal onto the basis function and the signal under study [24]. This method can be generalized to any transform estimation on unevenly sampled signals. Let $x(t)$ be the continuous signal under study and $b_i(t)$ an orthogonal basis set that defines the transform. It is well known that the coefficients $c(i)$ that represent $x(t)$ in the transform domain are

$$c(i) = \int_{-\infty}^{\infty} x(t) b_i(t)\, dt \tag{1}$$

and also that these coefficients $c(i)$ are those which minimize the squared error $e(c_i)$ defined in [26] as

$$e(c_i) = \int_{-\infty}^{\infty} (x(t) - c(i) b_i(t))^2\, dt. \tag{2}$$

When dealing with evenly sampled signals this formalism becomes its discrete counterpart, which in the case of the Fourier domain is well studied as the discrete time Fourier transform (DTFT), the discretely evaluated version (DFT) and the associated fast algorithm (FFT) used to compute it [27]. When the signal $x(t)$ is accessible only at unevenly spaced samples at t_n instants, the solution has generally been to reduce it to an evenly sampled signal through sampling interpolation. However, as stated in Section I, this resampling introduces some distortion in the spectrum (or transform) we are estimating (detailed analysis of this effect will be presented in Section II-C). To avoid this problem, Lomb [24] proposed to estimate the Fourier spectra of an unevenly sampled signal by adjusting the model

$$x(t_n) + \varepsilon_n = a\cos(2\pi f_i t_n) + b\sin(2\pi f_i t_n) \tag{3}$$

in such a way that the mean squared error ε_n is minimized with the proper a and b parameters. We can easily prove that this expression is a particularization for real signals from the more general

$$x(t_n) + \varepsilon_n = c(i) e^{j2\pi f_i t_n} \tag{4}$$

where now $x(t)$ and c can be complex valued. For any transform, not necessarily the Fourier transform, the expression will be

$$x(t_n) + \varepsilon_n = c(i) b_i(t_n). \tag{5}$$

Minimization of ε_n variance (mean squared error) leads to minimization of

$$\sum_{n=1}^{N} |x(t_n) - c(i) b_i(t_n)|^2 \tag{6}$$

which results in a value for $c(i)$

$$c(i) = \frac{1}{k} \sum_{n=1}^{N} x(t_n) b_i^*(t_n) \quad k = \sum_{n=1}^{N} |b_i(t_n)|^2. \tag{7}$$

This result can be referred to as a generalized Lomb method to estimate transforms of unevenly sampled data.

The signal power at index i of the transformation $(P_x(i))$ will be [24]

$$\begin{aligned} P_x(i) &= c(i) \sum_{n=1}^{N} x^*(t_n) b_i(t_n) = k \cdot |c(i)|^2 \\ &= |\hat{c}(i)|^2 \quad \text{with } \hat{c}(i) = c(i)\sqrt{k}. \end{aligned} \tag{8}$$

If the transform is the Fourier transform then $k = N$ and $P_x(i) = P_X(f) = \hat{c}^2(f)$. In the original work [24], Lomb introduces a delay at the basis ($\sin$ and $\cos$ rather than exponentials), which becomes in a more efficient estimation algorithm, the Lomb normalized periodogram.

$$\begin{aligned} P_X(f) = \frac{1}{2\sigma^2} \Bigg\{ & \frac{\left[\sum_{n=1}^{N} (x(t_n) - \bar{x}) \cos(2\pi f(t_n - \tau))\right]^2}{\sum_{n=1}^{N} \cos^2(2\pi f(t_n - \tau))} \\ & + \frac{\left[\sum_{n=1}^{N} (x(t_n) - \bar{x}) \sin(2\pi f(t_n - \tau))\right]^2}{\sum_{n=1}^{N} \sin^2(2\pi f(t_n - \tau))} \Bigg\} \end{aligned} \tag{9}$$

where $\bar{x}$ and σ^2 are the mean and variance of the data and the value of τ is defined as

$$\tan(4\pi f\tau) = \frac{\sum_{n=1}^{N}\sin(4\pi f t_n)}{\sum_{n=1}^{N}\cos(4\pi f t_n)}. \tag{10}$$

Later, in [28] and [29], a fast algorithm was presented to estimate the Lomb spectrum.

III. Frequency Analysis of the Lomb PSD Estimation Method

The remaining question of this PSD estimation method is, how is the original spectrum of the signal $x(t)$ ($|X(f)|^2$, where $X(f)$ is the Fourier transform of $x(t)$), related to the spectrum estimated using the Lomb method? To analyze this, we recover (7), and we see that it can be rewritten in a different way in terms of the Dirac function $\delta(t)$

$$\begin{aligned}\hat{c}(i) &= \frac{1}{\sqrt{k}}\sum_{n=1}^{N} x(t_n)b_i^*(t_n)\\ &= \frac{1}{\sqrt{k}}\int_{-\infty}^{\infty}\sum_{n=1}^{N} x(t)\delta(t-t_n)b_i^*(t)\,dt.\end{aligned} \tag{11}$$

We see that the coefficients obtained from the generalized Lomb method are those which come from the projection of the unevenly sampled signal $x_s(t) = \frac{1}{\sqrt{k}}\sum_{n=1}^{N} x(t)\delta(t-t_n)$ onto the base signal $b_i(t)$. In the particular case of the Fourier transform, this means that the Lomb spectrum is the spectrum of the continuous time unevenly sampled signal

$$x_s(t) = \frac{1}{\sqrt{N}}\sum_{n=1}^{N} x(t)\delta(t-t_n) \tag{12}$$

so, in fact, the Lomb spectrum is the $|X_s(f)|^2$ spectrum. Note that we have replaced k by N since the sum of $\sum_{n=1}^{N}|e^{i2\pi f t_n}|^2 = N$. The relationship between $X_s(f)$ and $X(f)$ will give the relationship between the estimated Lomb spectrum and the real one from the original signal.

Knowledge of the distribution of $X_s(f)$ requires knowledge of the t_n distribution, and this will depend on each application. In this work, we proposed and analyze two different models for the t_n distribution. First, we consider that the distribution of t_n series can be modeled (over stationary periods), as a uniform sampling with a random deviation. Second, we will consider that t_n can be modeled as uniform sampling with a sinusoidal deviation.

For signals like HR, the deviation of the uneven sampling from the uniform is not very large, at least over stationary periods, and then it will be possible to assume this approximations. The uneven sampling of the HR will probably not fit, exactly, either of these two models since from the integral pulse frequency modulation (IPFM) model [30] t_n comes from the integral of a band-limited modulating signal $m(t)$ that accounts for the cardiovascular autonomic control action on the HR. Even though these two models represent two opposite limit behaviors, the real t_n could be fitted somewhere between them. The behavior of the Lomb estimate in both models, for the case of small deviation from uniform sampling, is comparable (see Sections III-A and III-B), it can be extrapolated to real HR signals.

A. Sampling Modeled as Uniform Plus Random Variation

In this Section we consider the uneven sampling as uniform plus a random deviation. Then, t_n can be expressed as

$$t_n = n\cdot T - \alpha_n \tag{13}$$

where α_n is a random variable with zero mean and probability distribution function $P_{\alpha_n}(\alpha_n)$. The t_n distribution is supposed to satisfy $E[t_n - t_{n-1}] = T$ and $E[t_n - nT] = 0\ \forall n$ (for convenience, the origin of time has been selected at the origin of sampling). The sampled signal $x_s(t)$ becomes, in this case

$$x_s(t) = \frac{1}{\sqrt{N}}\sum_{n=1}^{N} x(t)\delta(t-nT+\alpha_n). \tag{14}$$

Moreover, $x(t)$ is assumed to be a deterministic signal to be estimated, the random variable α_n makes $x_s(t)$ a random process, therefore, its Fourier transform $X_s(f)$ is a random process. In this case we will consider the mean $E[X_s(f)]$ and the variance $\sigma_{|X_s(f)|^2}$ to have some information on how the estimated Lomb spectra $|X_s(f)|^2$ is related to the real signal spectrum $|X(f)|^2$.

1) Mean of the Lomb Spectrum Estimate: Applying the convolution theorem, we have that from (14)

$$X_s(f) = \frac{1}{\sqrt{N}}X(f) * \int_{-\infty}^{\infty}\sum_{n=1}^{N}\delta(t-nT+\alpha_n)e^{j2\pi ft}\,dt \tag{15}$$

and estimating the mean of this random process we have

$$\begin{aligned}\bar{X}_s(f) = E[X_s(f)] &= \frac{1}{\sqrt{N}}X(f)\\ &* \int_{-\infty}^{\infty}\sum_{n=1}^{N}\int_{\alpha_n}\delta(t-nT+\alpha_n)P_{\alpha_n}(\alpha_n)\,d\alpha_n e^{j2\pi ft}\,dt\end{aligned} \tag{16}$$

$$\begin{aligned}\bar{X}_s(f) &= \frac{1}{\sqrt{N}}X(f)\\ &* \int_{-\infty}^{\infty}\sum_{n=1}^{N}\delta(t-nT)\int_{\alpha_n} e^{-j2\pi f\alpha_n}P_{\alpha_n}(\alpha_n)d\alpha_n e^{j2\pi ft}dt\end{aligned} \tag{17}$$

where $P_{\alpha_n}(\alpha_n)$ is the probability density function of the random variable α_n. If we express this result as a function of the characteristic function $P_{\alpha_n}(f)$

$$P_{\alpha_n}(f) = \int_{\alpha_n} P_{\alpha_n}(\alpha_n)e^{-j2\pi f\alpha_n}\,d\alpha_n \tag{18}$$

we have

$$\bar{X}_s(f) = \frac{1}{\sqrt{N}}X(f) * \int_{-\infty}^{\infty}\sum_{n=1}^{N}\delta(t-nT)P_{\alpha_n}(f)e^{j2\pi ft}\,dt. \tag{19}$$

Assuming that the random variables α_n have the same probability distribution function (do not change with time) at each time instant t_n, $P_{\alpha_n}(f) = P_\alpha(f)$, the mean of the $X_s(f)$ function is

$$\bar{X}_s(f) = \frac{1}{\sqrt{N}} X(f) * \left[P_\alpha(f) \int_{-\infty}^{\infty} \sum_{n=1}^{N} \delta(t - nT) e^{j2\pi f t}\, dt \right] \tag{20}$$

$$\bar{X}_s(f) = \frac{1}{\sqrt{N}} X(f) * \left[P_\alpha(f) \left(f_s \sum_{n=-\infty}^{\infty} \delta(f - nf_s) * W(f) \right) \right] \tag{21}$$

where $f_s = 1/T$ is the mean sampling frequency, and $W(f)$ is the window Fourier transform of

$$w(t) = \begin{cases} 1, & t_1 < t < t_N \\ 0, & \text{otherwise.} \end{cases} \tag{22}$$

This expression now allows us to interpret $E[X_s(f)]$ in terms of the known uniform sampling Fourier transform [31]. $E[X_s(f)]$ is the convolution of the original Fourier transform signal $X(f)$ with the Fourier transform of a uniform sampling function windowed by the finite time observation interval $W(f)$ and now weighted by the characteristic function of the randomly distributed sampling $P_\alpha(f)$. Again the sampling theorem appears in order to avoid aliasing, where now, the Nyquist frequency comes from the mean sampling interval T. So, to have a correct estimate, the mean sampling frequency should be higher than twice the highest frequency of the signal $x(t)$. This agrees with the result from [10] that only if the maximum frequency component of the signal is lower than half the inverse of the mean sampling interval (mean heart period) the original signal can be recovered. The other ith frequency bands will represent (in mean) the repetition of the base band spectrum weighted by the value of the characteristic function $P_\alpha(i \cdot f_s)$ evaluated in multiples of the mean sampling function f_s. In the case that $P_\alpha(\alpha)$ is a Gaussian distribution with standard deviation σ, the characteristic function is [32]

$$P_\alpha(f) = e^{-\left(2\pi^2 f^2 \sigma^2\right)} \tag{23}$$

which consists of a low-pass filter with a cutoff frequency (f_c) at -3 dB of $f_c = 132.5/\sigma$, where f_c is expressed in Hz and σ in ms. Then the estimated mean base-band spectrum using the Lomb method is unbiased and each ith mean upper band will be affected by the factor $e^{-(2\pi^2 (i \cdot f_s)^2 \sigma^2)}$ that depends on the sampling distribution t_n through the σ value, and on band order i.

From this result we see that, in this kind of uneven sampling, an alias limit appears in the frequencies that can be recovered from the original signal. However, this study has been done with the mean Fourier transform $\bar{X}_s(f) = E[X_s(f)]$ and the Lomb estimate gets a single trial of this random process. This leads us to study the variance of the Lomb estimate to see how much a single trial estimate will differ from the mean value.

2) Variance of the Lomb Spectrum Estimate: To study the Lomb estimate variance we will first study the expected value of $|X_s(f) - \bar{X}_s(f)|^2$ which can be calculated as

$$\begin{aligned} &\overline{|X_s(f) - \bar{X}_s(f)|^2} \\ &\quad = E[(X_s(f) - \bar{X}_s(f))(X_s(f) - \bar{X}_s(f))^*] \\ &\quad = E[X_s(f) X_s(f)^*] - \bar{X}_s(f) \bar{X}_s(f)^*. \end{aligned} \tag{24}$$

In Appendix I a closed expression for this expected value is obtained, as shown in (25) at the bottom of the page.

In the case of a normal distribution $P_\alpha(f)$, and a band-limited signal $x(t)$, we can approximate this expression. The frequency content of $x(t)$ is zero for those frequencies higher than the Nyquist frequency $(X(f) = 0$ for $|f| > f_s/2)$. Then the integral in expression (25), affected by a $X(f - f')$ factor, needs to be calculated only at those frequencies f' which satisfy $f - f_s/2 < f' < f + f_s/2$. On the other hand, if we have the probability density function $P_\alpha(\alpha)$ concentrated in α, the characteristic function $P_\alpha(f)$ will be highly spread in frequency. We can consider that the standard deviation of the distribution σ is small compared with the mean sampling period $T, \sigma \ll T$ (usual situation in real cases like HR signals). If this is the case, and for f in the first frequency bands, we can approximate the characteristic function $P_\alpha(f')$ by its value at the nth integration band. With this approximation, and considering $P_\alpha(f)$ real and symmetric, since it comes

$$\begin{aligned} \overline{|X_s(f) - \bar{X}_s(f)|^2} = &\frac{1}{N} \int_{-\infty}^{\infty} -X(f - f') \left\{ X^*(f - f') * \left(P_\alpha(-f') \left[f_s \sum_{n=-\infty}^{\infty} \delta(f' - nf_s) * (W(f') * W(f')) \right] \right) \right\} df' \\ &- \frac{1}{N} \int_{-\infty}^{\infty} -X(f - f') P_\alpha(-f') \left\{ X^*(f - f') P_\alpha(f') * \left(f_s \sum_{n=-\infty}^{\infty} \delta(f' - nf_s) * (W(\hat{f}) * W(\hat{f})) \right) \right\} df' \end{aligned} \tag{25}$$

$$\begin{aligned} \overline{|X_s(f) - \bar{X}_s(f)|^2} = &\left(P_\alpha(nf_s) - P_\alpha^2(nf_s)\right) \\ &\times \frac{1}{N} \int_{-\infty}^{\infty} -X(f - f') \left\{ X^*(f - f') * \left[f_s \sum_{n=-\infty}^{\infty} \delta(f' - nf_s) * (W(\hat{f}) * W(\hat{f})) \right] \right\} df' \\ &nf_s - f_s/2 < |f| < nf_s + f_s/2 \end{aligned} \tag{26}$$

from a symmetric distribution function, (25) can be expressed as (26), shown at the bottom of the previous page. The integral multiplying factor can be approximated, neglecting the effect of the window function, by

$$\int_{-\infty}^{\infty} f_s X(f-f')X^*(f-f')(-df') = f_s \cdot \mathrm{SE} \tag{27}$$

where SE is the signal energy. With this approximation, we have an approximate expression for the expectation

$$\overline{|X_s(f)-\bar{X}_s(f)|^2} = \left(P_\alpha(nf_s) - P_\alpha^2(nf_s)\right)\frac{1}{N} f_s\,\mathrm{SE} \quad \text{with } nf_s - f_s/2 < |f| < nf_s + f_s/2. \tag{28}$$

However, the algorithm proposed by [29] performs a power normalization of the signal to be of unitary power $f_s\,\mathrm{SE}/N = 1$. Then we have

$$\overline{|X_s(f)-\bar{X}_s(f)|^2} = P_\alpha(nf_s) - P_\alpha^2(nf_s) \quad \text{with } nf_s - f_s/2 < |f| < nf_s + f_s/2. \tag{29}$$

In the special case of a normal distribution (23)

$$\overline{|X_s(f)-\bar{X}_s(f)|^2} = e^{-2\pi^2\sigma^2 n^2 f_s^2}\left(1 - e^{-2\pi^2\sigma^2 n^2 f_s^2}\right) \quad \text{with } nf_s - f_s/2 < |f| < nf_s + f_s/2 \tag{30}$$

and considering that $\sigma \ll T$

$$\overline{|X_s(f)-\bar{X}_s(f)|^2} = 2(\pi\sigma n f_s)^2 \quad \text{with } nf_s - f_s/2 < |f| < nf_s + f_s/2. \tag{31}$$

Analyzing this expression, we can see that the expectation $\overline{|X_s(f)-\bar{X}_s(f)|^2}$ increases with the deviation of the sampling σ, the band order and the sampling frequency.

However, the magnitude of interest is not the $\overline{|X_s(f)-\bar{X}_s(f)|^2}$ value, but the variance of $\hat{c}^2(f) = |X_s(f)|^2$. To estimate this variance $\sigma_{|X_s(f)|^2}$ we can proceed in the following way. From (24) we see that

$$E[|X_s(f)|^2] = E[X_s(f)X_s(f)^*] = E[X_s(f)]E[X_s(f)]^* + \overline{|X_s(f)-\bar{X}_s(f)|^2} \tag{32}$$

and assuming $|X_s(f)|$ to be a Gaussian process [33]

$$\sigma^2_{|X_s(f)|^2} = 4\overline{|X_s(f)|}^2\sigma^2_{|X_s(f)|} + 2\sigma^4_{|X_s(f)|}. \tag{33}$$

This expression is not known, but we can find an upper bound; from (24)

$$E[|X_s(f)|^2] = E[X_s(f)X_s(f)^*] = E[X_s(f)]E[X_s(f)]^* + \overline{|X_s(f)-\bar{X}_s(f)|^2} = \overline{|X_s(f)|}^2 + \sigma^2_{|X_s(f)|} \tag{34}$$

that leads to the following inequalities

$$\overline{|X_s(f)|} < \sqrt{E[X_s(f)]E[X_s(f)]^* + \overline{|X_s(f)-\bar{X}_s(f)|^2}} \tag{35}$$

$$\overline{|X_s(f)|}^2 \geq E[X_s(f)]E[X_s(f)]^* \text{ implying } \Longrightarrow \sigma^2_{|X_s(f)|} \leq \overline{|X_s(f)-\bar{X}_s(f)|^2} \tag{36}$$

$$\sigma^2_{|X_s(f)|^2} \leq \left(4E[X_s(f)]E[X_s(f)]^* + 6\overline{|X_s(f)-\bar{X}_s(f)|^2}\right) \times \overline{|X_s(f)-\bar{X}_s(f)|^2}. \tag{37}$$

Now we are in a position to evaluate

$$E\left[|X_s(f)|^2\right] = E[X_s(f)X_s(f)^*] = E[X_s(f)]E[X_s(f)]^* + 2(\pi\sigma n f_s)^2 \quad \text{with } nf_s - f_s/2 < |f| < nf_s + f_s/2 \tag{38}$$

which at the base-band $(n = 0)$ is an exact estimate of the PSD of $X(f)$, and

$$\sigma_{|X_s(f)|^2} \leq 2\sqrt{E[X_s(f)]E[X_s(f)]^* + 3(\pi\sigma n f_s)^2}\sqrt{2(\pi\sigma n f_s)^2} \tag{39}$$

which again becomes zero for the base-band and certificates the single trial Lomb estimate as a correct estimate of the PSD of $x(t)$ signal. Note that the deviation also increases with the value of the spectrum at a given frequency. If the signal is evenly sampled $(\sigma = 0)$, we recover the spectrum of the classic uniformly sampled signals. As the band order increases, $n > 0$, the estimate is a biased estimate and its variance increases with the band order, the sampling frequency, and the dispersion of the sampling.

B. Sampling Modeled as Uniform Plus Sinusoidal Variation

Now we consider the uneven sampling as uniform plus a sinusoidal deviation. Then, t_n can be expressed as

$$t_n = n \cdot T - \Delta(t_n) \tag{40}$$

where $\Delta(t_n)$ is a sinusoidal function $\Delta(t) = b\sin(2\pi f_m t)$. The sampled signal $x_s(t)$ becomes, in this case

$$x_s(t) = \frac{1}{\sqrt{N}}x(t)\sum_{n=1}^{N}\delta(t - nT + \Delta(t_n)) = \frac{1}{\sqrt{N}}x(t)w(t)s(t) \tag{41}$$

being $w(t)$ the window function defined in (22) and

$$s(t) = \sum_{n=-\infty}^{\infty}\delta(t - nT + \Delta(t_n)) \tag{42}$$

the unevenly spaced sampling function. The Fourier transform $X_s(f)$ is

$$X_s(f) = \frac{1}{\sqrt{N}}X(f) * S(f) * W(f) \tag{43}$$

and requires knowledge of $s(t)$ to be evaluated and analyzed.

A detailed analysis of $s(t)$ signal shows that it represent a problem equivalent to the problem of *pulse position modulation (PPM)* that appears at modulation systems [31]. In [31] it is shown that

$$s(t) = f_s[1 + \dot{\Delta}(t)]\left\{1 + \sum_{k=1}^{\infty} 2\cos[2\pi k f_s t + 2\pi k f_s \Delta(t)]\right\} \tag{44}$$

when the condition $|\dot{\Delta}(t)| < 1$ is satisfied. Analyzing this condition for sinusoidal modulation, we have that $\dot{\Delta}(t) = b2\pi f_m\cos(2\pi f_m t)$. Taking f_m a frequency lower than 0.5

Hz (situation in HR signals) and $|b| \ll T \approx 1$ s (equivalent to consider the deviation from uniform sampling small (40) and a mean HR of around 60 bpm), we have that the condition is satisfied and the analysis is correct. Each one of the addition terms in (44) is a phase modulation component that, when the modulating signal $\Delta(t)$ is a sinusoid, becomes in a cosine expansion with the first kind Bessel functions, $J_n(x)$, [31]

$$\cos(2\pi f_s t + a\sin(2\pi f_m t)) = \sum_{n=-\infty}^{\infty} J_n(a)\cos(2\pi f_s t + 2\pi n f_m t). \quad (45)$$

When (45) is substituted in (44) for $\Delta(t) = b\sin(2\pi f_m t)$ ($f_m < 0.5$ and $|b| \ll 1$) it appears an expansion for $s(t)$ as follows:

$$s(t) = f_s[1 + b2\pi f_m \cos(2\pi f_m t)] \times \left\{1 + 2\sum_{n=-\infty}^{\infty}\sum_{k=1}^{\infty} J_n(2\pi k f_s b) \times \cos(2\pi k f_s t + 2\pi n f_m t)\right\}. \quad (46)$$

Using the properties of the Bessel functions this expression can also be compacted to

$$s(t) = f_s + f_s 2\pi f_m b\cos(2\pi f_m t) + \sum_{n=-\infty}^{\infty}\sum_{k=1}^{\infty} 2f_s J_n(2\pi k f_s b)\left(1 + \frac{nf_m}{kf_s}\right) \times \cos(2\pi k f_s t + 2\pi n f_m t). \quad (47)$$

Now we have an expansion of the $s(t)$ signal in terms of sinusoidal functions that can be represented in the frequency domain. The obtained expression is in agrement with that obtained in [34] for a spectrum of counts with the difference that in that work the modulating signal $\Delta(t) = b\sin(2\pi f_m t)$ is first passed through the IPFM model and then it appears the integration constants differences. In the frequency domain $S(f)$ becomes

$$S(f) = f_s\delta(f) + f_s\pi f_m b(\delta(f - f_m) + \delta(f + f_m)) + \sum_{n=-\infty}^{\infty}\sum_{k=1}^{\infty} f_s J_n(2\pi k f_s b)\left(1 + \frac{nf_m}{kf_s}\right) \times (\delta(f - kf_s - nf_m) + \delta(f + kf_s + nf_m). \quad (48)$$

Then, from (43), the $X_s(f)$ spectrum becomes

$$X_s(f) = \frac{1}{\sqrt{N}} f_s X(f) * W(f) * \left[\delta(f) + \pi f_m b(\delta(f - f_m)\delta(f + f_m)) + \sum_{n=-\infty}^{\infty}\sum_{k=1}^{\infty} f_s J_n(2\pi k f_s b)\left(1 + \frac{nf_m}{kf_s}\right) \times (\delta(f - kf_s - nf_m) + \delta(f + kf_s + nf_m)\right]. \quad (49)$$

This expression allows again to interpret the $X_s(f)$ spectrum as function of the original spectrum $X(f)$. It appears that the spectrum is the convolution of the original with the window function and then convolved with $S(f)$. $S(f)$ represents a weighted Dirac delta repetition with the mean sampling frequency f_s plus harmonics of the frequency f_m used at the uneven sampling. These harmonics, at bands above the base band, are infinity with decreasing values; and at the base band (the one of interest) appears a unique contaminating harmonic at f_m. This $S(f)$ function is represented in Fig. 1 for values of $f_s = 1$ Hz (equivalent, in HR signals, to a mean HR of 60 bpm), $b = 0.1$ (that corresponds in HR signals to HR variations from 66.6 to 54.5 bpm), and f_m =0.1, 0.15 and 0.2 Hz (that are typical frequencies at the HR modulating signals). The contamination at the base band could suppose a problem except when the Dirac delta amplitude $(f_s\pi f_m b)$ at frequency f_m is negligeable with respect to the unitary amplitude of the fundamental delta. In Fig. 1 we see that for the values referring the typical situations in HR signals ($b = 0.1$, $f_s = 1$, and $f_m = 0.15$), the delta amplitude is 0.04. If this value is considered in power, as usually is the PSD of HR signals, we have a ratio of $2 \cdot 10^{-3}$ that represents 27 dB lower influence of this contamination respect to the fundamental and then can be neglected. Simulation, in Section III-C, will corroborate this reasoning. The upper bands of the $X_s(f)$ spectrum $(k > 0)$ incorporate an attenuation respect to the base band (phenomenon also obtained when the uneven sampling was random) and higher-amplitude harmonics of the f_m frequency. Also, these harmonics $(|n| > 0)$ could extend to collateral bands but weighted by higher-order Bessel functions (J_n) that would make them gradually vanish. However, if the mean sampling frequency becomes low and the sinusoidal sampling variation frequency f_m high, those harmonics can be introduced at the base band, as already can be noted in Fig. 1 for $f_m = 0.15$ and 0.2 Hz. For our purposes this contamination at the base band is even more negligible than the previously commented (Fig. 1), and the Lomb estimate becomes a practically unbiased estimate of the original signal spectrum at the base band.

All these results are in agreement with those obtained for random sampling. We get same frequency repetition of the spectrum and the conclusion that only frequencies up to the mean sampling frequency can be recovered. The spectrum estimation at the base band can be considered the true spectrum except for factors whose influence is lower than around 27 dB and then can be neglected. In addition, the phenomenon of attenuation at the upper bands spectral repetition is also observed and the increase in variance observed at random model can be assimilated to the increase in harmonic contamination as the band order increases in the sinusoidal model. Note that again when the sampling approaches to the uniform $(b \to 0)$ the spectrum becomes the uniform spectrum. Thus, the Bessel function argument vanishes and its value goes to one when $n = 0$ and to zero when $n \neq 0$ for any band order k.

If in the model there were two tones instead of one, a new series of harmonics of the new frequency will be added to each delta of the single tone model spectrum [31]. When the model is not based on tones, but on a band-limited

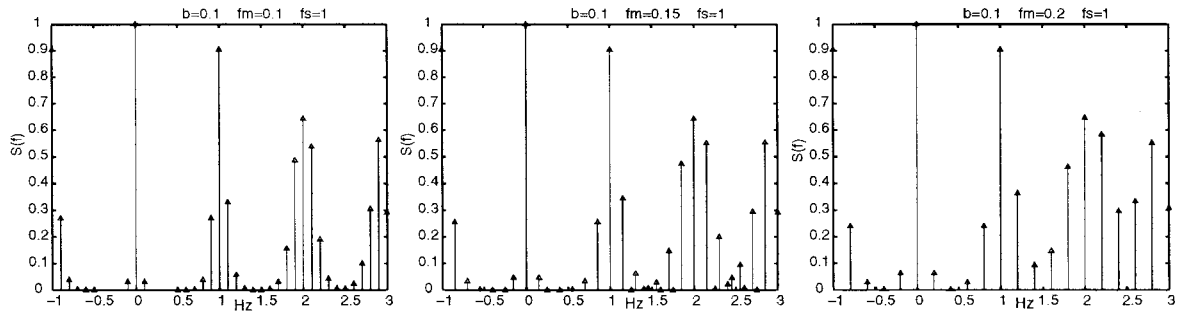

(a) (b) (c)

Fig. 1. Spectrum $S(f)$ for $b = 0.1$, $f_s = 1$ Hz and three different values of f_m. f_m = (a) 0.1, (b) 0.15, and (c) 0.2 Hz.

signal $b\Delta(t)$, $|\Delta(t)| < 1$, the problem is similar to that addressed at FM modulating systems [31] were the spectrum is estimated to spread significantly around each of the kf_s center frequency bands a value of $B_T(k) = (2\beta + 1)W$ (β the FM modulating index and W the maximum frequency component at the band-limited modulating signal). So, the lowest frequency that spreads the first band (f_l) is around $f_l = f_s - (\beta + 1/2)W$, that particularizing in our case with the identification of $\beta = 2\pi k f_s b$ in (44) [31] and the used values of $b = 0.1$, $k = 1$, $f_s = 1$ and $W = 0.35$ Hz (order of the maximum expected modulation component at HR signals) becomes $f_l = 0.6 > F_s/2 = 0.5$. This agrees with the spectrum obtained for the sinusoidal model, where it was shown that the base band spectrum (up to 0.5 Hz in this case) is not substantially contaminated by the first band components. At the base band will remain the desired zero frequency Dirac delta with the contamination of $\dot{\Delta}(t)$ (44) that (supposing variations of medium frequency range $W =$ 0.2 Hz) gets a relative value of $2\pi W b = 0.12$, implying 18-dB contamination that is negligeable when measuring the PSD indexes of HRV.

C. Simulation Results

To test the extent and validity of previous derivations we have designed two different experiments: First a controlled Gaussian $x(t) = e^{-t^2/100}$ sampled at 100 Hz and extended during 1000 s (16.67 min) has been generated. The spectrum of this signal is also a Gaussian with a cutoff frequency at -3 dB of $f_c = 0.0132$ Hz. Then, this spectrum will be adequate to test if the predictions of previous section are satisfied. Once the signal is computer generated at a sampling rate of 100 Hz, it has been unevenly subsampled with a mean sampling frequency $f_s = 1$ Hz and variations (random and sinusoidal). The random case takes sampling instants that differ from the uniform in a α_n value in $[-b/2 = -0.05, b/2 = 0.05]$ s uniformly distributed, and the sinusoidal case takes $b = 0.1$ and $f_m = 0.15$ Hz to model the sampling variations according to the expression given in (40). Also, it has been considered a random noise added to the signal to emulate the real HR signals where the RR interval estimation has the limit of the original sampling frequency of the ECG [15], $x(t)$ is then $x(t) = e^{-t^2/100} + rand$ with *rand* a uniform random variable in $[-0.02, 0.02]$ s, emulating the noise in a HR signal from ECG sampled at 250 Hz. The spectrum of the resulting uneven subsampled signal is presented in Fig. 2. The right panels show the spectra up to 4 Hz that include four bands of the original signal spectrum with a mean sampling rate of $f_s = 1$ Hz. The left panels show the counterparts of the right panels, but up to 2 Hz to have a detail of the base and first band. In Fig. 2(a) we have the original spectrum of the signal (without added noise) uniformly sampled at 1 Hz. This is the "ideal" spectrum that we will try to obtain from the uneven sampled signal. Fig. 2(d) shows its counterpart when noise is added to the signal. Fig. 2(b) shows the Lomb estimates when the uneven subsampling follows the sinusoidal model and there is not added noise. These estimates agree with (49) where it appears the spectrum repetition with the mean sampling frequency $f_s = 1$ Hz. It appears the harmonic at the base band at frequency $f_m = 0.15$ with a relative magnitude respect to the main component of less that 27 dB as predicted. Analyzing the first band (right panel) we see the predicted repetitions with respect to the f_s with the f_m value and amplitudes according to the values estimated in (49). At upper bands we also corroborate the attenuation of the main lobe amplitude. Extra low level peaks appeared around 0.5 Hz, not clearly predicted by the model; however looking at Fig. 2(e) (which includes the added noise in the original signal), we see that this peak falls at the level of the noise given by rounding the sampling instant to one sample of the original Gaussian signal. Fig. 2(c) and (f) shows the Lomb estimates when the subsampling is random; (c) for clean signal, and (f) for the noise one. Again the prediction obtained at the random model (unbiased estimate at base band and low-pass filtering at upper bands) is corroborated. The characteristic function $P_\alpha(f)$ becomes in this case $P_\alpha(f) = ((1/0.1)(\sin(2\pi f 0.05))/\pi f)$ which gives a cutoff frequency $f_c \geq 4.5$ Hz, implying around 6-dB attenuation at the lobe of the fourth band, as can be observed in panels (c) and (f). In conclusion, both models considered for uneven sampling obtain predictable results modeled by our derivations. Other subsampling will fit somewhere between the two models and it is predictable that the results will not differ substantially with those presented in this simulation. Results with HR data will corroborate this in Section IV.

Previous simulation has corroborated the prediction about the analytical deviations for the Lomb estimates. Also, we have obtained that, even in a low degree, the Lomb estimate presents some contamination in the base-band that could affect the spectrum estimation in real practice. To corroborate this

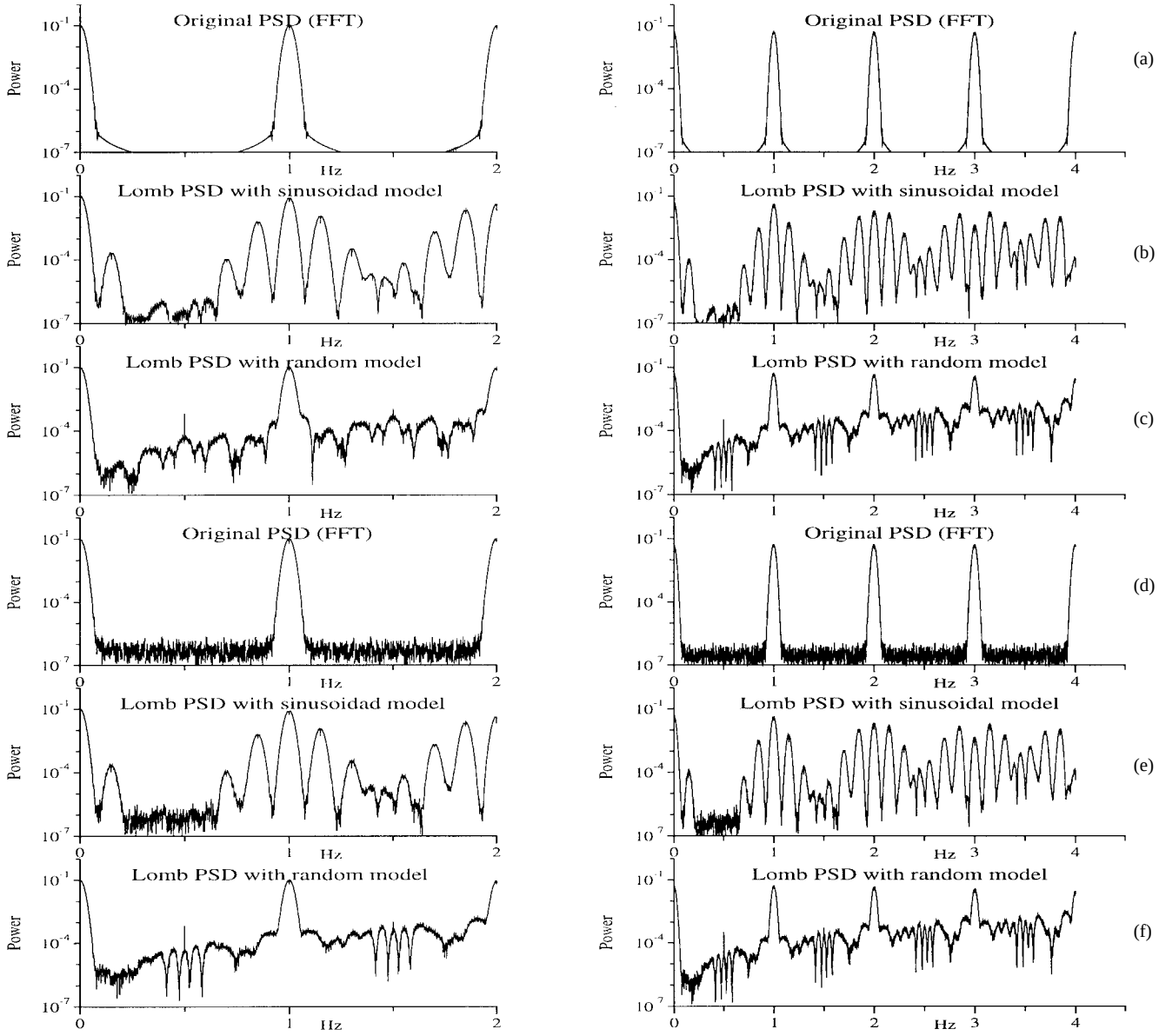

Fig. 2. Simulated spectrum estimations: $f_s = 1$ Hz, $b = 0.1$, and $fm = 0.15$. Original and Lomb estimated spectrum of a Gaussian signal unevenly subsampled. Right panels show the spectrum in four bands and left panels, a detail in the base-band and first repetition band. (a) The original spectrum, (b) the Lomb estimate when the subsampling follows the sinusoidal model, and (c) the Lomb estimate when the subsampling follows the random model. (d)–(f) Refit (a)–(c) when the original Gaussian signal is contaminated by noise. See text for detailed discussion.

result we have designed a simulation generating a Gaussian-like signal with the aim to emulate standard spectrum in HRV studies. The simulated $x(t)$ signal is

$$x(t) = e^{-(t-25)^2/40} + 0.9e^{-(t-125)^2/40}\cos(2\pi 0.15t) + 0.8e^{-(t-225)^2/40}\cos(2\pi 0.3t). \quad (50)$$

The signal is originally sampled at 100 Hz and then unevenly subsampled as described in previous simulations, and also the noise to emulate the QRS detection error in HR signals has been added. The subsampling is made with several f_s values, b parameter values, and f_m frequencies. Also, the spectrum estimated using interpolation (linear and cubic splines) at time domain to get a uniform sampling before FFT is applied has been obtained.

In Fig. 4 we present the results for $f_s = 1$ Hz (mean HR of 60 bpm), $b = 0.1$ (variations from 55.5 to 66.5 bpm) and $f_m = 0.13$ (modulating signal of that frequency). The panels on the left represent the base band spectrum estimated up to 0.5 Hz and the right panels show the same spectrum up to 1 Hz. In Fig. 4 (a) it is represented the original spectrum if the signal were uniformly sampled at 1 Hz and then is the "ideal" spectrum to be estimated. In panel (b) we have overprinted on the original spectrum (dotted line), the spectrum estimated with FFT after interpolation resampling to 1 Hz (linear interpolation is solid line and cubic spline interpolation is dashed line). We see how this classical technique of estimating the PSD suffers of a low-pass filtering of the spectrum. This phenomenon is higher for linear than for splines interpolation, as can be easily explained from the filtering theory.

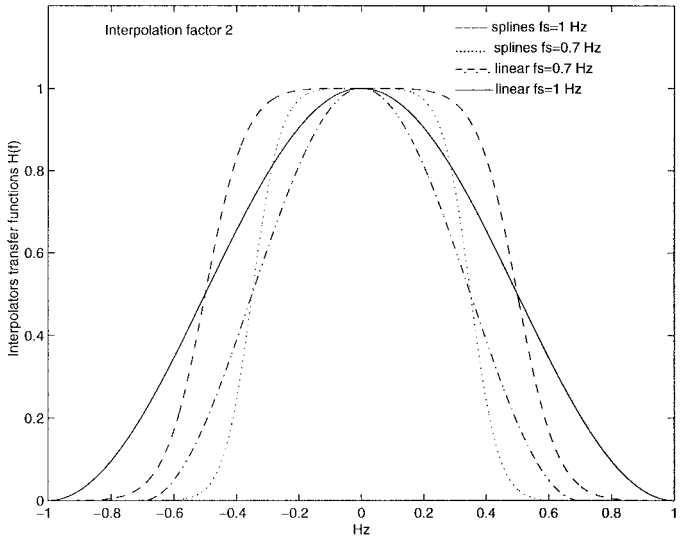

Fig. 3. Transfer function of the interpolating filters for linear and cubic spline interpolation. The functions are for interpolation factor of two, in cases of $f_s = 1$ and 0.7 Hz. Note how the low-pass filtering is higher when the period between samples increases (f_s decreases). Also, it is evident that the cubic spline achieves better behavior than the linear interpolation.

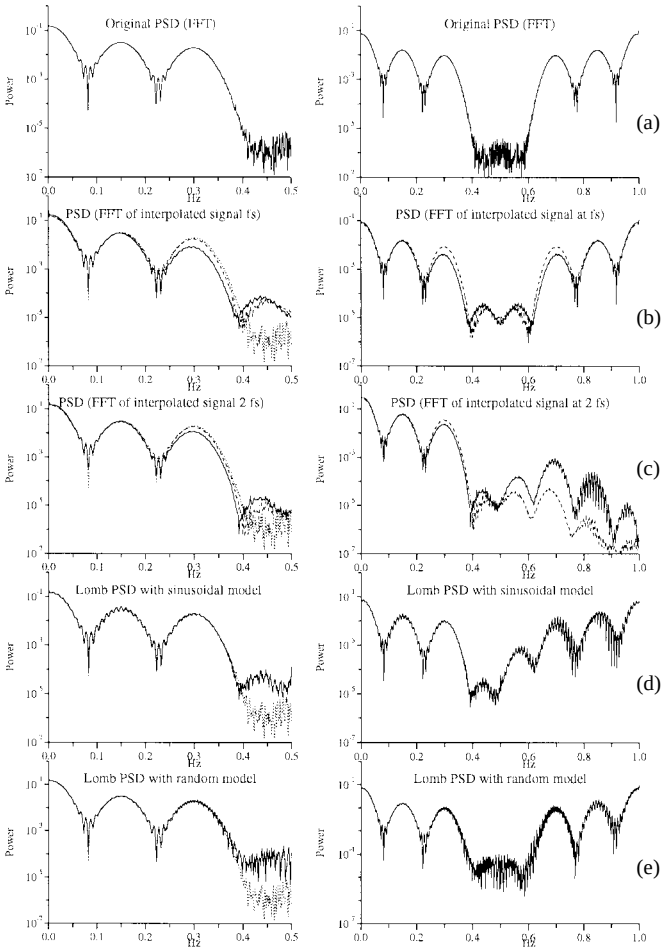

Fig. 4. Spectrum estimations for a signal formed by three Gaussian. Panels on the left show the spectrum up to $f_s/2 = 0.5$ with dotted overprinted of the original spectrum in (a). Panels on the right show the expanded spectrum up to $f_s = 1$ Hz. (a) The original spectrum uniformly sampled at 1 Hz. (b) The spectra estimated after interpolation (linear solid line, cubic spline dashed line) to uniform sampling at 1 Hz. (c) The same as (b), but interpolating to 2 Hz. (d) The Lomb estimates when the uneven subsampling is sinusoidal with $b = 0.1$ Hz and $f_m = 0.13$ Hz. (e) The Lomb estimates when the uneven subsampling is random with $b = 0.1$ Hz. See text for comments on the results.

The interpolation is a low pass-pass linear filter whose frequency response can be calculated by doing the FFT of the impulse response when interpolating a signal valued one at one sample and zero at the rest (impulse response). This calculation can be analytically done for linear interpolation obtaining a transfer function of $H(w) = (1/L)\left[\sin^2(wL/2)/\sin^2(w/2)\right]$ (w is normalized frequency and L is the order of the interpolation). The cutoff frequency of this filter can be numerically obtained and we get a -3-dB cutoff frequency $f_c = 0.32 f_s$ Hz (it has a minor dependence with L at low L values (from $0.36 f_s$ to $0.32 f_s$) that is not relevant in our study). The cutoff frequency for cubic splines interpolation has been calculated empirically, constructing the impulse response, and we have obtained a $f_c = 0.42 f_s$ Hz that is larger than in case of linear interpolation. Fig. 3 represents the transfer functions for these filters in case of $f_s = 1$ and 0.7 Hz, where we see that the cutoff frequencies are those given previously and that the spline interpolation has a much better behavior than the linear for the same data. However, in unevenly sampled signals, the interpolation is not a linear time-invariant filter, but a linear time-varying filter, since the period between samples where the interpolation is done varies, and the f_c frequency also varies. Then we have considered the cutoff frequency corresponding to the mean interval period $(1/f_s)$ as the mean cutoff frequency. This approximation will work if the variation from even sampling is not high, as is always being considered in this study.

Going back to Fig. 4(b), we corroborate the expectation from the filter transfer functions previously discussed. The panels in (b) are obtained with resampling to 1 Hz that can be seen as resampling to 2 Hz [Fig. 4(c)] plus a decimation to 1 Hz. This is important since the estimation in (b) has a higher contamination lobe around 0.43 Hz than the estimation in (c) has (resampled at 2 Hz). This is explained because when we decimate from 2 Hz to 1 Hz [going from (c) to (b)], it appears to be an aliasing at frequencies around 0.5 Hz that increases the contamination at high frequencies. So, even the original signal frequency content does not exceed 0.4 Hz, it is advisable to do the resampling at higher frequencies (at least 2 Hz). We can continue with this interpretation looking now at panel (d) where there is the Lomb estimate with sinusoidal variation. We see that at the base band the estimate does not suffer from the low pass effect (also, the original spectrum is overprinted in dotted line on the left). It appears a peak at around 0.43 Hz that corresponds to the convolution of the original spectrum with the contaminating delta at f_m in the base band ($f_m = 0.13$, plus 0.3 Hz of the upper Gaussian contribution yield 0.43 Hz that coincides with the peak occurrence). This peak is about 30 dB lower than the main signal components at the base band and then negligible, but we realize that is in agreement with the peaks observed in panels (b) and (c) with the resampled signal. This is because the resampling is done on the unevenly sampled signal that intrinsically contains the Lomb spectrum (spectrum of the unevenly sampled signal) and the low-pass

effect of the resampling attenuates these extra peaks if they are at frequencies higher than the corresponding interpolator cuttoff frequency. We see in Fig. 4(d) that the Lomb estimate is a very good estimate of the original spectrum, where the signal has components and at high frequencies introduces the predicted extra peaks, also included at the interpolation estimates, but Lomb avoiding the low-pass effect. Even though cubic splines interpolation [Fig. 4(c)] gets a very close estimate to the original spectrum, this will degrade as the f_s value decreases, as can be seen in next simulation. Finally, Fig. 4(e) shows the result of estimating the Lomb spectrum when the subsampling is random, obtaining same conclusion as before, except that now the peak at 0.43 Hz is not clearly marked. This is predictable, since at the random model we do not have an explicit reconstruction of the interfering term, however, the results obtained from a general modulating signal and FM band estimation, in which the first band contamination does not come to the base band with significative values, can still can be applied. In panel (e) the high-frequency contamination at 0.5 Hz is at least 25 dB lower than the useful component. In both cases, the Lomb estimate obtains an unbiased estimate of the original spectrum in opposition to the resampled estimate (left panels).

To test the Lomb estimate in different situations than those described in previous experiments, we have considered $f_s = 0.7$ Hz (heart rate of 42 bpm) $b = 0.2$ (heart rate variations from 50 to 75 bpm assuming a mean of 60 bpm) and $f_m = 0.22$ Hz and several combinations of these values. In Fig. 5 we have the results in four different cases. In all of them we have overprinted in dotted line the original spectrum up to the mean Nyquist frequency; in subpanels a) the spectrum, interpolating to the mean sampling period with linear (solid line) and cubic splines (dashed line) are drawn, in subpanels b) are their counterpart resampling to two times the mean sampling frequency, subpanels c) represent the Lomb estimates with the sinusoidal model and in d) the Lomb estimates with the random model. Low heart rates $f_s = 0.7$ (42 bpm) are in Fig. 5(a) where we see the large effect of the low-pass filtering introduced by interpolation (both linear and splines), see Fig. 3, and the much better performance obtained by the Lomb estimates. Large variations in HR ($b = 0.2$ s) are shown in Fig. 5(b) where we see that the low-pass effect is higher than in Fig. 4 even when the f_s and f_m are the same. This is due to the time varying property of the interpolation of uneven sampled signals, since now there are more intervals spaced up to 1.2 s. The low-pass effect in those areas is more important, and the total low-pass effect obtained in subpanels a) and b) of Fig. 5(b) is higher than the obtained in Fig. 4 for $b = 0.1$, again cubic splines performs closely to Lomb estimates. Large modulation frequency $f_m = 0.22$ Hz, is analyzed in Fig. 5(c) with the only remarkable effect that the 0.43-Hz peak of Fig. 5(b) is delayed to the right, as is expected from the theoretical derivations. Note that the resampling to $2f_s$ gives lower aliasing at frequencies above 0.4 Hz (see peak amplitude) as stated in previous simulation and Fig. 5(c). Finally, all effects together have been considered in Fig. 5(d): Mean HR of 42 bpm, maximum variation from 36–49 bpm, and large frequency of uneven sampling variation. Again we corroborate the superior performance of the Lomb estimate with no low-pass effect. The oscillation that appears at the estimates is remarkable. However, since the clinical indexes are integral indexes on the spectrum, no substantial effect will be induced in opposition with the low-pass filtering that will strongly bias the indexes. This will be analyzed in Section IV.

In conclusion, we have obtained that the Lomb estimate, is not a unbiased estimate at the base band, but under the conditions that appears at HR related signals, the contamination is negligible and of much less magnitude than that introduced by the resampling required by FFT or AR-based methods. For HR over 60 bpm, interpolation with cubic splines approaches the Lomb estimate and, if the HR increases over these values, both spectra can be considered adequate estimates for frequencies up to 0.4 Hz. The interpolation techniques can not avoid the high-frequency spectral contaminations introduced by the uneven sampling, but they attenuate the frequencies with the low-pass filtering effect, that for this contribution becomes a positive effect. Further studies on interpolators that keep the low frequencies, and more drastically attenuate the high frequencies, will lead to better estimated of the underlying HRV signal spectrum.

IV. Analysis of Heart Rate Spectrum

In this Section we will analyze some spectra of HR series. In the first case we will perform a simulation to establish the improvement of the Lomb method with controlled HR signals. Afterwards we will consider real ECG records where the stationarity of the data is well satisfied (random deviation over uniform sampling). For this purpose we consider HR data from paced patients, which strictly guarantees the stationarity of data, and from patients with nearly stationary HR. In the last part of this Section we analyze the spectrum of HR series, not necessarily stationary, and interpret the results of previous Sections for these cases.

A. Application to Simulated Heart Rate Signals

To experimentally study the performance of the Lomb PSD estimate, we have found that real HR signals are not adequate since we do not know the real spectra that we want to obtain. We obtain different estimations from classical and Lomb estimates, but we cannot argue which is a better estimate from an experimental point of view. The theory already proves this.

To avoid this problem, we propose the following experiment [17], which uses the IPFM model [30] to generate the beat occurrence times from a modulating signal $m(t)$ that represents the sympathetic and parasympathetic influences on the sino-atrial node. The beat occurrence times are related to the modulating signal $m(t)$ as

$$k = \int_0^{t_k} \frac{1 + m(t)}{T}\, dt \tag{51}$$

where k is an integer representing the order of kth beat and T is the mean of the RR interval. The PSD estimates try to infer the spectral characteristics of $m(t)$ from the accessible information at beat occurrence times t_k. We generate beat series from a controlled $m(t)$ signal following a typical

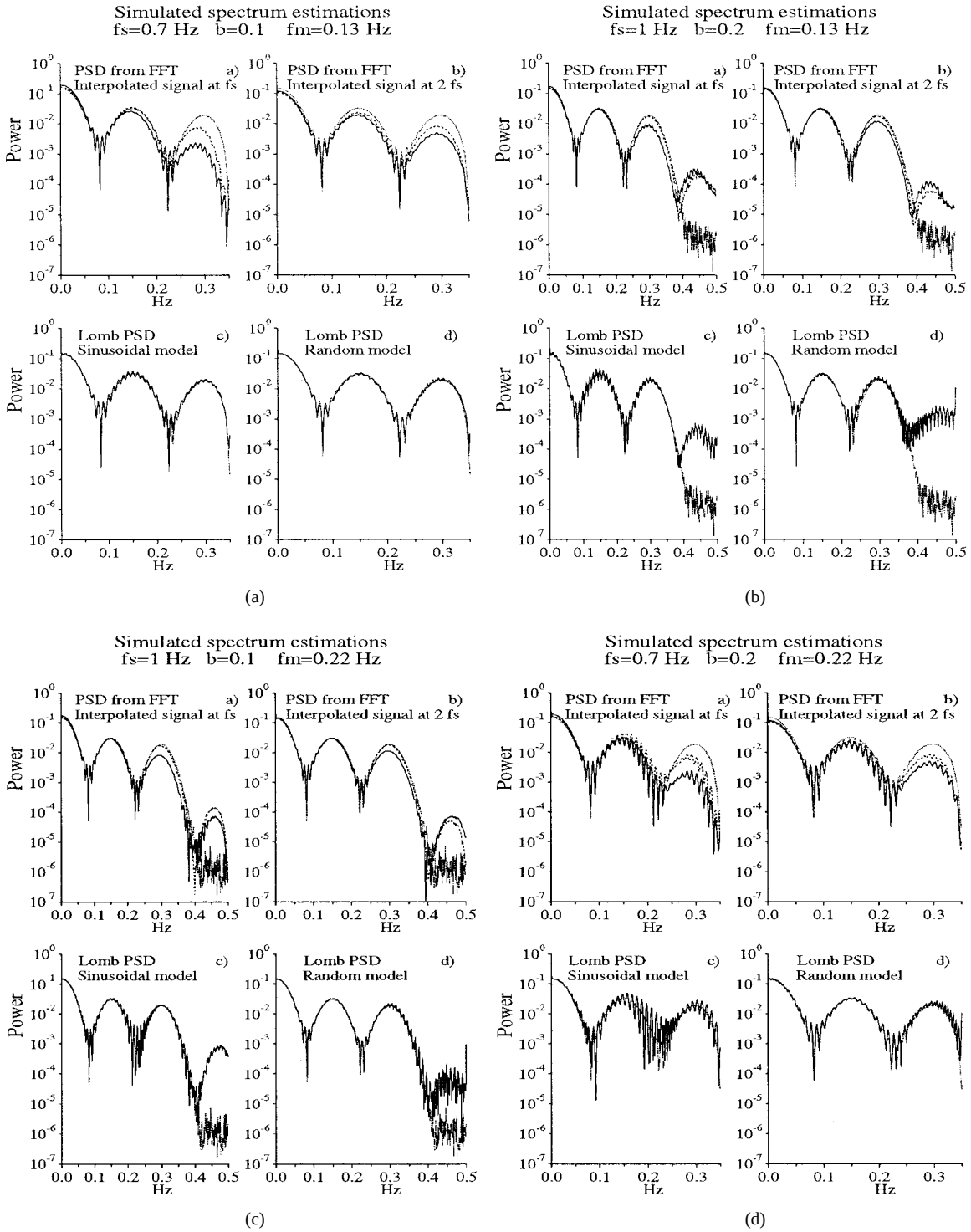

Fig. 5. Simulations of Fig. 4 in different conditions of mean HR, variation from the mean and modulating frequency. (a) Low HR, (b) large variation from the mean HR, (c) large modulating frequency, and (d) all together. Subpanels a) and b) have overprinted the original spectrum (dotted line), and those estimated with linear (solid line) and cubic spline (dashed line) interpolations. Subpanel a) is after resampling to the mean sampling frequency f_s and b) to two times that frequency. Subpanels c) and d) have the Lomb estimates (solid line) overprinted with the original spectrum (dotted line).

spectrum from a real subject. We have used the nine-order AR model proposed in [35] for generating sequences of $m(n)$ signal, as

$$m(n) = \sum_{k=1}^{P} a_k m(n-k) + n(n) \tag{52}$$

where a_k are the AR parameters shown in Table I, P is the AR model order and $n(n)$ is white zero-mean noise with standard deviation $\sigma_n = 0.072$ that results in a standard deviation of $m(n)$ signal, $\sigma_m = 0.145$. The value used for the sampling frequency is 1 Hz. In Fig. 6(a), (b) is the amplitude spectrum corresponding to this model.

The $m(n)$ signal, after being interpolated a factor of 16 (resulting sampling rate of 16 Hz), is the input to the IPFM

TABLE I
COEFFICIENTS OF THE AR MODEL USED TO GENERATE THE MODULATING SIGNAL $m(n)$ WHEN EXCITED BY WHITE NOISE

a_1	a_2	a_3	a_4	a_5	a_6	a_7	a_8	a_9
1.0701	- 0.3360	- 0.0117	-0.0758	0.4281	-0.2354	-0.1165	0.0119	0.1435

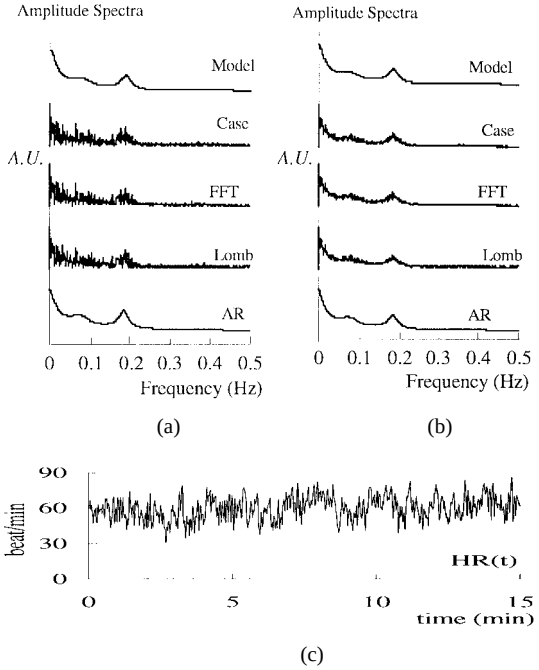

Fig. 6. (a) Model amplitude spectrum, the amplitude spectrum of a case (for a given noise realization) of the $m(n)$ signal, and the spectra obtained from FFT, AR, and Lomb estimates. (b) Mean amplitude spectra averaged in eight realizations for eight different noise $n(n)$ realizations. (c) Heart rate signal in a particular realization.

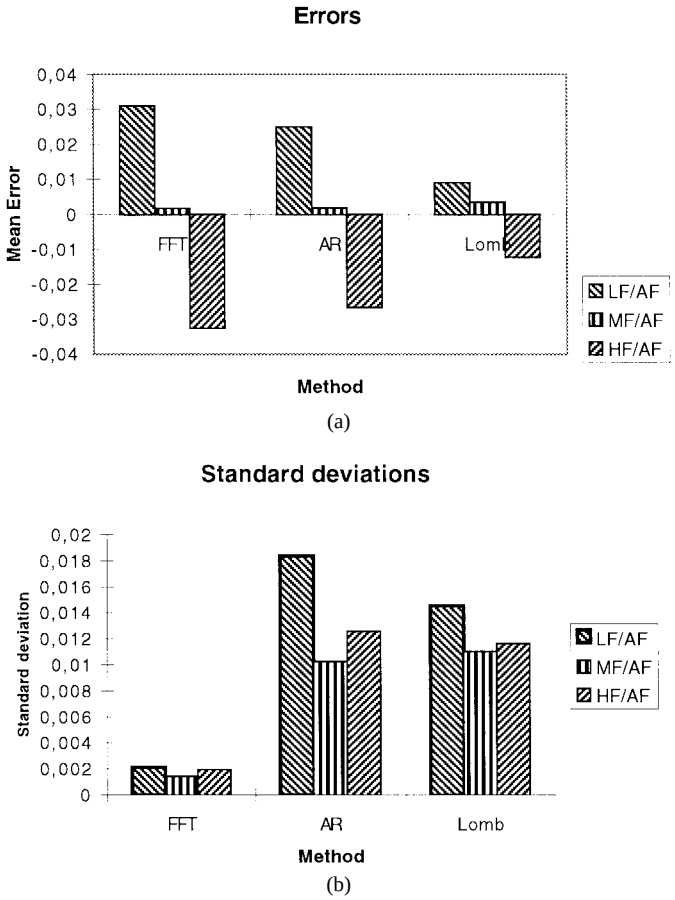

Fig. 7. (a) Mean and (b) standard deviation of the error in each band. Note that the values are referred to the unity since the bands energy is normalized.

model for obtaining the sequence of the beat occurrence times. We generate 1024 beats with mean heart period $T = 1$ s in the IPFM model. Fig. 6(c) shows a HR signal corresponding to this model. Then, we apply three methods for PSD estimation: FFT of interpolated HR signal with cubic splines at regularly spaced samples of 1 s; AR estimation of the previous interpolated HR signal with a nine-order model; Lomb estimate of the unevenly spaced HR signal. Fig. 6(a) shows the model amplitude spectrum, the amplitude spectrum of a case (for a given noise realization) of the $m(n)$ signal, and the spectra obtained from FFT, AR, and Lomb estimates. In Fig. 6(b) the mean amplitude spectra averaged in eight realizations for eight different noise $n(n)$ realizations are shown. The PSD is frequently divided into three bands of frequency: LF (0.01–0.08 Hz), MF (0.08–0.15 Hz), and HF (0.15–0.5 Hz) to get the clinical indexes. We have calculated the relative power LF/AF, MF/AF and HF/AF, where $\mathrm{AF} = \mathrm{LF} + \mathrm{MF} + \mathrm{HF}$, to compare each method of spectral estimation with the original spectrum of $m(n)$ in each case. Then, we have calculated the error in each band as the difference between the relative power obtained with each method and that obtained from the corresponding realization of $m(n)$. Finally, in Fig. 7 we present the mean of the error (ME) and the standard deviation (σ) in eight different realizations. In Fig. 7, we can see that the interpolated methods (FFT and AR estimates) have a strong low-pass response, since the error is positive at the LF band and negative at the HF band. The Lomb method is the one with the best behavior, since the error is lower and more equally distributed throughout the entire frequency band. This simulation corroborates our theoretical expectations that the Lomb estimate attenuates the low-pass effect generated by the resampling required by the classical methods (FFT, AR).

B. Application to Stationary Real Heart Rate Signals

In Fig. 8(a) we have the HR series of a paced patient from record 102 of the MIT-BIH ECG database [36]. The data presents the 15-min HR series starting at minute 6 of the 102 record. In this record an artifactual peak was introduced in the frequency domain (0.167 Hz) due to a nonsymmetric capstan used in the playback system [36]. This artifact and its harmonics will serve in this study as the test for the Lomb PSD method. In this case, the HR is very stable with very small variations and the assumption of stationary

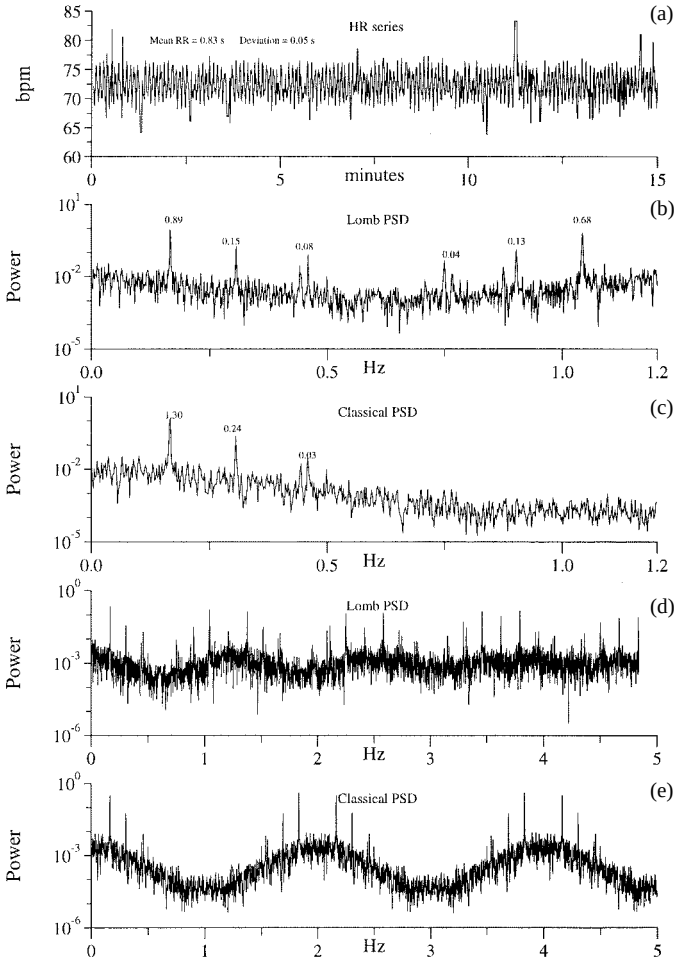

Fig. 8. Spectral analysis of HRV from record 102 of MIT-BIH database. (a) The HR series, (b) the Lomb spectrum in two "mean" Nyquist frequencies, and (c) classical spectrum after uniform resampling of the data at 2 Hz; (d) and (e) are the same as b and c for higher frequency values to evidence the spectra periodicity.

uneven sampling is well satisfied. Fig. 8(b) displays the Lomb spectra of this data where we have rejected noise and ectopic beats with the procedure presented in [23]. Fig. 8(c) displays the spectrum estimated through resampling the data at a sampling frequency of 2 Hz and estimating the spectrum with classical periodogram with FFT. In uniformly sampled signals, the Lomb method is equivalent to the classical periodogram estimated with FFT algorithms [24], [25]. The mean sampling frequency in the original HR series is 1.21 Hz and the deviation is 31 ms. In Fig. 8(d) and (e), the same spectra are displayed, but over a wider frequency range in order to show the periodicity at the different bands.

Analyzing the Lomb spectrum, we corroborate that there appears a periodicity whose period is the mean sampling frequency, 1.21 Hz, as predicted by the study in Section III. There appear in the spectrum three harmonically related peaks at 0.16, 0.30, and 0.45 Hz which correspond to the artifact introduced by the capstan. We can note [Fig. 8(b)] how these peaks have lower amplitude in the second band (0.6–1.8 Hz) than in the primary ($-$0.6–0.6 Hz) as a result of the low-pass effect introduced by the deviation of the uneven sampling. In Fig. 8(d) we have the Lomb spectrum for several cycles of the mean sampling frequency 1.21 Hz. We can corroborate the periodic behavior of this spectrum with the mean sampling frequency and the low-pass effect given by the sampling dispersion at the upper bands. Note that the peaks and mean shape of the signal at higher bands have lower amplitude, and that the signal becomes more embedded by the noise and the spectrum deviation.

Considering now, the spectrum obtained from resampling and classical spectrum estimation [Fig. 8(e)], we note that the spectrum has the expected 2-Hz (sampling frequency) periodicity, and also note [Fig. 8(c)] that the spectrum at high frequencies is attenuated as a result of the resampling. This is particularly evident at the third peak of the spectrum, which is somewhat less marked than in the Lomb spectrum. Also, note that because of the constant power normalization, an attenuation of high-frequency components results in an amplification of low-frequency components. The effect of high-frequency attenuation introduced by the resampling is particularly important in the HRV analysis, where the ratio between the energy at different bands is used as a clinical marker of cardiac dysfunction [8]. Thus, we verify the theoretical prediction that the Lomb spectral estimate is better than the resampled spectral estimate.

The highest significant frequency that we should consider in the spectrum of this uneven sampling of data is that corresponding to half the mean sampling frequency. This is an intuitive result in signals like HR series where the discrete nature of the signal is presumed not to have frequencies higher than the intrinsic frequencies at which they are generated.

The previous spectral study was repeated using the HR series of a nonpaced patient (normal situation for these studies), and the results are presented in Fig. 9. The patient corresponds to record e0125 of the European ST-T ECG database [37], and we analyzed the first 15 min of the record. The mean sampling frequency is in this case 1.18 Hz with a deviation of 30 ms, which is comparable to that of the previous example. Analyzing the spectrum, we recognize a frequency component around 0.33 Hz that is generally accepted to be related to respiratory modulations of the HR affected via the parasympathetic nervous system [18]. Again, we corroborate the results of the previous example with some new remarks. In Fig. 9(c), a spectral contribution around 0.83 Hz appears in the classical spectrum; however from Fig. 9(b) we note that only frequencies up to 0.59 (half of 1.18 Hz) are significant. The origin of the 0.83-Hz contribution in the classical spectrum, Fig. 9(c), is due to the resampling at 2 Hz that recovers contents up to 1 Hz of the original signal. In this case, the original signal, because of the mean sampling frequency at 1.18 Hz has a repetition spectrum from 0.59 Hz that gives an harmonic at 0.83 Hz $<$ 1 Hz, and then it is recovered at the base band of the resampled spectrum introducing an undesired artifact. Again, we corroborate that the resampling attenuates the high frequencies since this artifact has lower energy than it does in the original signal, Fig. 9(b)–(e).

Analyzing the periodicities of the spectra, Fig. 9(d) and (e), we note the same behavior in the Lomb spectrum as in the previous example, but now the frequency contents of the

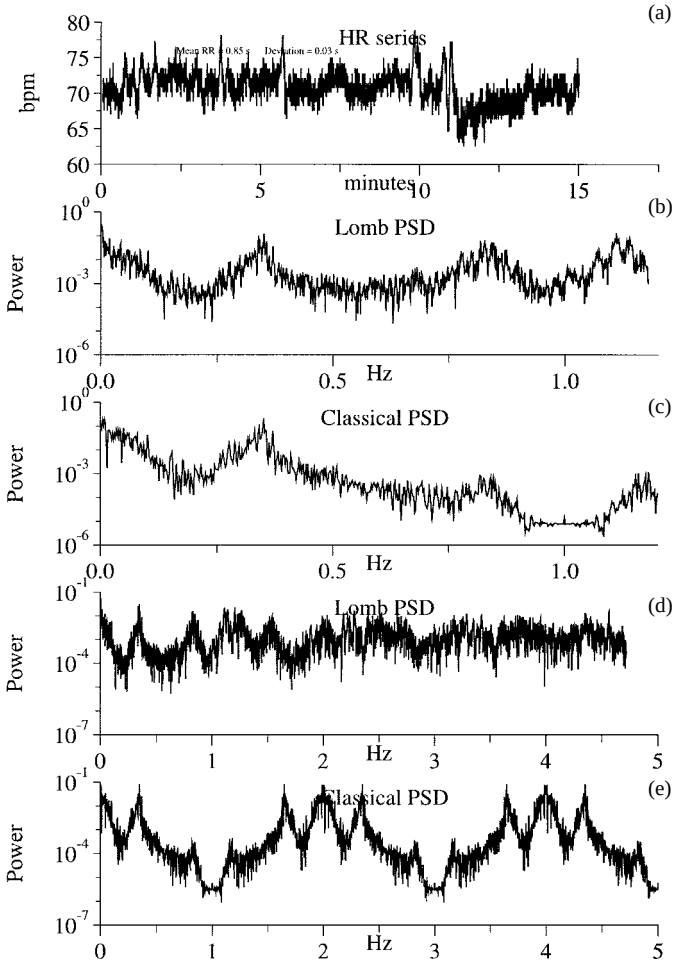

Fig. 9. Spectral analysis of HRV from record e0125 of European ST-T database. Same notation as in previous figure.

respiratory activity become unremarkable after the third band; even the sampling dispersion is comparable to the sample dispersion shown in previous example. This is due to the low power amplitude of this component compared with the peaks in Fig. 8; therefore, the low-pass effect makes them indistinguishable from the noise at a lower band order.

This study corroborates the theoretically predicted behavior of the Lomb spectral estimation method. We have shown its advantages compared to classical spectral estimation with resampling: namely, avoiding the high-frequency attenuation and extra periodic spectral repetitions (because resampling) that appear in classical methods at base band. Thus, we conclude that the Lomb method produces a better spectral estimate for unevenly sampled signals than those methods based on resampling.

C. Spectrum Interpretation in Nonstationary Signals

In this Section, we analyze the spectra when the uneven sampling is not stationary, meaning that we can not model the sampling as uniform modified by a random or sinusoidal deviation. Consider a signal $x(t)$ $(0 < t < t_0)$ sampled between $(0 < t < t_1)$ by a stationary, uneven sampling process with mean sampling frequency f_1; and between $(t_1 < t < t_0)$ by a different stationary, uneven sampling process with mean frequency f_2. We then have

$$x(t) = x_1(t) + x_2(t) \begin{cases} x_1(t) & = \begin{cases} x(t), & 0 < t < t_1 \\ 0, & \text{otherwise} \end{cases} \\ x_2(t) & = \begin{cases} x(t), & t_1 < t < t_0 \\ 0, & \text{otherwise} \end{cases} \end{cases} \tag{53}$$

where $x_1(t)$ and $x_2(t)$ come from a stationary, band-limited, unevenly sampled signals multiplied by the window function $w(t)$. The result is a time-limited signal of infinite bandwidth, but this effect has been modeled by the $w(t)$ and $W(f)$ functions, and so, the original signal can be considered bandlimited without loss of generality. We can, then apply the results of the previous Section. From (53) we can express the PSD of $x(t)$ as

$$|X(f)|^2 = |X_1(f) + X_2(f)|^2. \tag{54}$$

We know that the Lomb PSD estimate of $x(t)$, $|X_s(f)|^2$ will come from the square of the sum of $X_{1s}(f)$ and $X_{2s}(f)$ and will demonstrate the periodic behavior expected of the sum of two periodic spectra of different periods. For this reason, the highest frequency that will not be distorted by the periodicity will be half the smaller "average" sampling frequency, f_1 or f_2.

This result can be generalized to an arbitrary signal $x(t)$ with nonstationary sampling, dividing $x(t)$ into segments short enough to be considered stationary. Then the highest frequency in the Lomb spectra that will be free of aliasing will be half the smaller "average" sampling frequency in the stationary partitions. In terms of HR signals, this corresponds to the lowest HR of the patient during the analyzing period.

An excellent real-world example is shown in Fig. 10, which presents the results of the HR spectrum of a patient with abnormal atrioventricular (AV) conduction, with periods of 2 : 1 AV block. Note that if the objective of studying HRV were to examine autonomic nervous system control, one would want to analyze the spectrum of atrial rate variability. This ECG signal comes from record 231 of the MIT-BIH database. This pathology results in periods where the ventricular beat appears once for every two atrial beats. Then, when the HR series is constructed from a ventricular QRS detector, its rate during 2 : 1 block will be approximately half the rate of that occurring during periods with no AV block. In Fig. 10(a), a 15-min HR series of this record is displayed, where two episodes of 2 : 1 AV block (low HR) and two of normal rhythm (high HR) appear.

In Fig. 10(b), we show the Lomb spectrum of the 15-min HR series, where we note a signal attenuation as the frequency increases, but not a clear periodicity. Fig. 10(d) shows the Lomb spectrum of HR series between $2'40''$ and $6'30''$, which corresponds to the low HR period (AV block) with a mean sampling frequency of 0.6 Hz. The periodicity of this spectrum has been marked by "A." In Fig. 10(e), the same is shown for the high HR period between $6'40''$

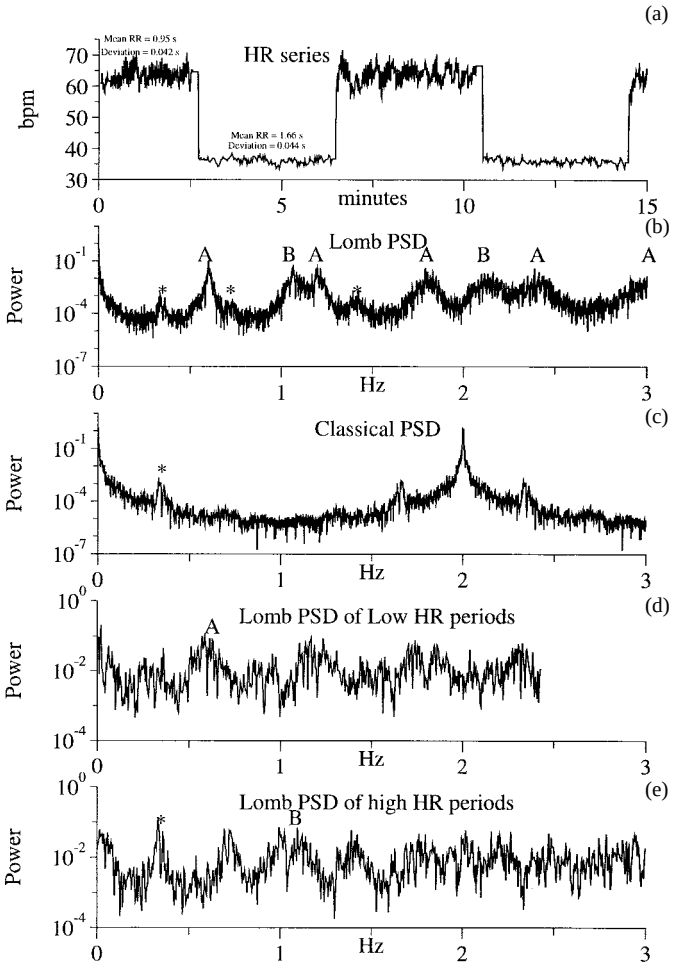

Fig. 10. Spectral analysis of HRV from record 231 of MIT-BIH database. (a) Shows the HR series, (b) is the Lomb spectrum, and (c) classical spectrum after uniform resampling of the data at 2 Hz. (d) Lomb spectrum of the HR series at the low HR period between 2'40'' and 6'30'' (values outside this interval have not been considered) and (e) Lomb spectrum of the HR series at the high HR period between 6'40'' and 10'20''.

and 10′20″, with a mean sampling frequency of 1.05 Hz. In this case, a respiration-related peak marked by "*" and the periodicity with the mean sampling frequency marked "B" appear. Going back to Fig. 10(b) we realize that it is composed of the superposition of two signals, of periodicities "A" and "B." Also, the respiration-related peaks "*" appear with the repetitions associated with the "B" periodicity (high HR) to which they are related. In this way, we corroborate that the Lomb spectrum in this case is the superposition of two signals, each one affected by its own periodicity. In this case, the highest frequency with no aliasing is 0.3 Hz. However, since the spectrum of the low HR has no significant contribution at the high frequencies, the respiratory contribution of the high HR at frequencies >0.3 Hz is preserved without important distortion in the spectrum shown in Fig. 10(b).

Two more observations can be made from the spectra in Fig. 10. First, the low-frequency contribution has a much higher contribution in the Lomb spectra of the whole HR signal, Fig. 10(b), than it does in the Lomb spectrum of each separate period, Fig. 10(d), (e). This effect is a result of the mean signal subtraction that is performed prior to estimating the Lomb spectrum [24]. In the case where the whole signal is taken, the mean is some intermediate value between the low and high mean HR. This results in a signal with an important dc and low-frequency components, whereas this does not happen when averaging the low or high HR periods independently. This effect, even considering only the spectrum up to the lower "mean" Nyquist frequency, will alter the ratio between the low and the high-frequency contents; this ratio is used in clinical diagnosis. Also, as shown in Fig. 10(c), we can note the artifactual contribution of low frequencies and the respiratory-related peak at frequencies belonging to the second band of the high HR spectrum. This problem, in patients with gradually changing stationarity (no this case) can be attenuated by detrending the HR series (set its mean first derivative to zero). This is equivalent to subtracting a best-fit (by least squares) line from the HR series.

In a general signal with no clearly divided stationary periods, the study will be analogous. The highest frequency free of aliasing will be half the lower mean sampling frequency in the stationary partitions of the HR signal. The effect of the relatively high low-frequency contents will, again, appear as a result of the nonstationarity, which keeps the mean subtracted HR series with the low-frequency contamination. This is important in HRV analysis, as has been previously stated, making it necessary to select a HR time period with as stable behavior as possible to have an artifact-free HR spectrum.

V. Conclusion

In this work we have presented a detailed analysis of the Lomb method for power spectrum estimation of unevenly sampled signals. We have developed analytical expressions to find the performance of the estimate and we have corroborated this study applying the Lomb power spectrum estimation to HR signals.

In particular, we have noted that when the uneven sampling can be modeled as uniform with random variations or sinusoidal, the Lomb spectrum repeats itself with the mean Nyquist frequency, being an unbiased estimate of the signal power spectrum in the base band and with a low-pass effect at upper bands that depends on the sampling distribution or the sinusoidal variation. In addition, when the dispersion of the sampling with respect to the uniform one is small, the deviation of the Lomb estimate at the base band, with respect the true spectrum, is negligible.

Our theoretical predictions about the Lomb spectral estimation were confirmed experimentally using simulated and real HR series signals. Comparison to the classical PSD estimation method applied after resampling demonstrated the limitations of the resampling approach and the superior performance of the Lomb estimate which avoids the low pass effect of resampling and prevents about the introduction of artifactual components in the base-band due to the inadequate consideration of the highest frequency up to which the base-band extends. We have found a periodic behavior of the Lomb spectrum, which corresponds to the frequency of the mean sampling period. We conclude that the upper significant

frequency without aliasing is half the mean Nyquist frequency (that corresponding to the mean HR), and that signals with frequency components higher than this will be affected by aliasing.

The simulation with Gaussian-like signals has agreed the theoretical results, showing the superior performance of the Lomb estimate with respect to the resampled estimates. This effect is more remarkable as the mean sampling frequency becomes smaller (heart rhythms lower than 60 bpm) where the resampling supposes superior low-pass effect that is avoided by Lomb estimations. For higher heart rhythms (superior to 60 bpm) the Lomb estimate behaves better that linear resampling, but the estimation with cubic spline interpolation approaches that of the Lomb estimate as the mean HR frequency increases. However, both the Lomb estimate and the resampled estimates can introduce some high-frequency contamination when either the variations from uniform sampling are dramatic or the frequency of the variation is very high. This circumstance is very unlike over stationary HR signals, where the PSD of HRV estimation should be done. This contamination is a inherent problem of the uneven sampled signals, that can be addressed with the help of superior performance interpolators that keeping the low frequencies, more drastically attenuate the high-frequency parts in a selective way. Also, to avoid aliasing, it has been shown that the resampling should be done at least to double the mean sampling frequency that in HR signals can be fixed around 2 Hz.

We have analyzed the case of uneven sampling that does not follow the uniform plus random sampling patterns. In these cases we have found that the highest frequency without aliasing in the Lomb spectrum is that frequency corresponding to the lowest mean sampling rate in any portion of the original signal. This was corroborated in a HR signal from a patient with intermittent 2 : 1 AV block where there were two clearly differently sampled parts of the HR signal. This result is in total agreement with the theoretical analysis of unevenly sampled signals presented in [10].

We have demonstrated that the Lomb method provides better estimates of the HR spectrum than classical estimates. Since the power ratio between low- and high-frequency components is relevant in clinical diagnosis, the low pass effect introduced by the resampling in classical methods is not desirable. In addition, we have noted that the classical spectral estimation can include high-frequency components not present in the original signal, but due to periodicities of the original uneven sampled signal spectrum. These artifactual contributions can again alter the high/low power ratio and distort the spectral estimation. We also pointed out that spectral analysis of nonstationary HR series by any method will produce distortions which result from the impossibility of subtracting the dc level from the mean HR value. One possible way to attenuate this artifact is by detrending the series (set its mean first derivative to zero), that is equivalent to subtracting a best-fit (by least squares) line from the input data. The results of HRV analysis in nonstationary periods is an artifactual increase in low-frequency power which is unrelated to HRV. This problem can only be totally solved by analyzing the HR series during periods of stable mean HR.

APPENDIX I
DERIVATION OF A CLOSED EXPRESSION FOR $\overline{|X_s(f)-\bar{X}_s(f)|^2}$

To analyze the expectation of $\overline{|X_s(f)-\bar{X}_s(f)|^2} = E[|X_s(f)-\bar{X}_s(f)|^2$, we will express $X_s(f)$ as

$$X_s(f) = \frac{1}{\sqrt{N}} X(f) * \int_{-\infty}^{\infty} \sum_{n=1}^{N} \delta(t-nT) e^{j2\pi f \alpha_n} e^{j2\pi f t}\, dt = \frac{1}{\sqrt{N}} X(f) * Y(f) \tag{55}$$

where

$$Y(f) = \int_{-\infty}^{\infty} \sum_{n=1}^{N} \delta(t-nT) e^{j2\pi f \alpha_n} e^{j2\pi f t}\, dt \tag{56}$$

is a random process whose expected value is $E[Y(f)] = P_\alpha(f)[f_s \sum_{n=-\infty}^{\infty} \delta(f-nf_s) * W(f)]$.

To estimate $\overline{|X_s(f)-\bar{X}_s(f)|^2}$

$$\begin{aligned}\overline{|X_s(f)-\bar{X}_s(f)|^2} &= E[(X_s(f)-E[X_s(f)])(X_s(f)-E[X_s(f)])^*] \\ &= E[X_s(f)X_s^*(f)] - E[X_s(f)]E[X_s(f)]^*\end{aligned} \tag{57}$$

we need to estimate $E[X_s(f)X_s^*(f)]$ which becomes

$$\begin{aligned}E[X_s(f)X_s^*(f)] =& \frac{1}{N} E\left[\int_{-\infty}^{\infty} X(f-f')Y(f')\, df' \right. \\ & \left. \times \int_{-\infty}^{\infty} X^*(f-f'')Y^*(f'')\, df''\right] \\ =& \frac{1}{N} \int_{-\infty}^{\infty}\int_{-\infty}^{\infty} X(f-f')X^*(f-f'') \\ & \times E[Y(f')Y^*(f'')]\, df''\, df'\end{aligned} \tag{58}$$

then we need to estimate the $E[Y(f')Y^*(f'')]$ which from (56) can be expressed as

$$\begin{aligned}E[Y(f')Y^*(f'')] =& \\ & E\left[\int_{-\infty}^{\infty}\int_{-\infty}^{\infty} \sum_{n=1}^{N}\sum_{m=1}^{N} \delta(t-nT) e^{j2\pi f'(\alpha_n + t)} \right. \\ & \left. \times\, \delta(t'-mT) e^{-j2\pi f''(\alpha_m + t')}\, dt\, dt'\right].\end{aligned} \tag{59}$$

Assuming that the α_n are statistically independent for different time instants n the cross terms in the previous expression will appear only when $n = m$ and then

$$\begin{aligned}E[Y(f')Y^*(f'')] &= \sum_{n=-\infty}^{\infty}\sum_{m=-\infty}^{\infty} P_\alpha(-f')P_\alpha(f'')[\delta(f'-nf_s) \\ &\quad * W(f')][\delta(f''-mf_s) * W^*(f'')] \\ &\quad + \sum_{n=-\infty}^{\infty} (P_\alpha(-f'+f'') - P_\alpha(-f')P_\alpha(f'')) \\ &\quad \times \int_{-\infty}^{\infty} \delta(t-nT)W(t)e^{j2\pi f' t}\, dt \\ &\quad \times \int_{-\infty}^{\infty} \delta(t'-nT)W(t')e^{-j2\pi f'' t'}\, dt'\end{aligned} \tag{60}$$

$$\overline{|X_s(f)-\bar{\bar{X}}_s(f)|^2} = \frac{1}{N}\int_{-\infty}^{\infty}\int_{-\infty}^{\infty} X(f-f')X^*(f-f'')\sum_{n=-\infty}^{\infty}(P_\alpha(-f'+f'')-P_\alpha(-f')P_\alpha(f'')) \times W^2(nT)e^{j2\pi f' nT}e^{-j2\pi f'' nT}\,df'\,df'' \tag{61}$$

$$\overline{|X_s(f)-\bar{\bar{X}}_s(f)|^2} = \frac{1}{N}\int_{-\infty}^{\infty}\int_{-\infty}^{\infty} X(f-f')X^*(f-f'')(P_\alpha(-f'+f'')-P_\alpha(-f')P_\alpha(f'')) \times\left[f_s\sum_{n=-\infty}^{\infty}\delta(f'-f''-nf_s)*(W(f'-f'')*W(f'-f''))\right]df'\,df'' \tag{62}$$

$$\overline{|X_s(f)-\bar{\bar{X}}_s(f)|^2} = \frac{1}{N}\int_{-\infty}^{\infty}\int_{-\infty}^{\infty} X(f-f')X^*(f+\hat{f}-f')(P_\alpha(-\hat{f})-P_\alpha(-f')P_\alpha(\hat{f}+f')) \left[f_s\sum_{n=-\infty}^{\infty}\delta(\hat{f}-nf_s)*(W(\hat{f})*W(\hat{f}))\right]df'\,d\hat{f} \tag{63}$$

$$\overline{|X_s(f)-\bar{\bar{X}}_s(f)|^2} = \frac{1}{N}\int_{-\infty}^{\infty} -X(f-f')\left\{X^*(f-f')*\left(P_\alpha(-f')\left[f_s\sum_{n=-\infty}^{\infty}\delta(f'-nf_s)*(W(f')*W(f'))\right]\right)\right\}df' - \frac{1}{N}\int_{-\infty}^{\infty} -X(f-f')P_\alpha(-f')\left\{X^*(f-f')P_\alpha(f')*\left(f_s\sum_{n=-\infty}^{\infty}\delta(f'-nf_s)*(W(f')*W(f'))\right)\right\}df' \tag{64}$$

Introducing this result in [58], we obtain a first term that is equal to $\overline{E[X_s(f)]E[X_s(f)]^*}$, and the expected value $\overline{|X_s(f)-\bar{\bar{X}}_s(f)|^2}$ becomes as shown in (61) and (62) at the top of the page. Taking the variable change $f'-f''=\hat{f}$, we have (63) and (64), shown at the top of the page.

ACKNOWLEDGMENT

The authors would like to thank the referees who from their comments improved the paper, J. García for his detailed reading of the paper, and J. Mateo for his help with the simulated HR signals.

REFERENCES

[1] Task Force of The ESC/ASPE, "Heart rate variability: Standards of measurement, physiologically interpretation, and clinical use," *Ann. Noninvasive Electrocardiol.*, vol. 1, no. 2, pp. 151–181, Apr. 1996.
[2] M. Malik and A. J. Camm, *Heart Rate Variability*. New York: Futura, 1995.
[3] R. E. Klieger, J. P. Miller, J. T. Bigger, and A. J. Moss, "Decreased heart rate variability and its association with increased mortality after myocardial infarction," *Amer. J. Cardiol.*, vol. 59, pp. 256–262, 1987.
[4] S. Akselrod, D. Gordon *et al.*, "Power spectrum analysis of heart rate fluctuations: A quantitative probe of beat-to-beat cardiovascular control," *Science*, vol. 213, pp. 220–222, 1981.
[5] B. Pomerantz, R. J. B. Macaulay *et al.*, "Assessment of autonomic function in humans by heart rate espectral analysis," *Amer. J. Physiology*, vol. 248, pp. H151–153, 1985.
[6] M. Pagani, F. Lombardi *et al.*, "Power spectral analysis of heart rate and arterial pressure variabilities as a marker of sypatho-vagal interaction in man and conscious dog," *Circ. Res.*, vol. 59, pp. 178–193, 1986.
[7] T. J. van den Akker, A. S. M. Koeleman, L. A. H. Hogenhuis, and O. Rompelman, "Heart rate variability and blood pressure oscillations in diabetics with autonomic neuropathy," *Automedica*, pp. 201–208, 1983.
[8] G. A. Myers, G. J. Martin, N. M. Magid, P. S. Barnett, J. W. Schaad, J. S. Weiss, M. Lesch, and D. H. Singer, "Power spectral analysis of heart rate variability in sudden cardiac death: Comparison to other methods," *IEEE Trans. Biomed. Eng.*, vol. BME-33, pp. 1149–1156, Dec. 1986.
[9] D. Gordon, V. L. Herrera *et al.*, "Heart-rate spectral analysis: A noninvasive probe of cardiovascular regulation in critically ill children with heart disease," *Pediatric Cardiol.*, vol. 9, pp. 69–77, 1988.
[10] J. L. Yen, "On nonuniform sampling of bandwidth-limited signals," *IRE Trans. Circuit Theory*, vol. CT-3, pp. 251–257, Dec. 1956.
[11] A. J. Jerry, "The Shannon sampling theorem. Its various extensions and applications: A tutorial review," in *Proc. IEEE*, vol. 65, pp. 1565–1596, Nov. 1977.
[12] R. W. DeBoer, J. M. Karemaker, and J. Strackee, "Spectrum of a series of point event, generated by the integral pulse frequency modulation model," *Med. Biol. Eng. Comput.*, vol. 23, pp. 138–142, 1985.
[13] R. D. Berger, S. Akeselrod, D. Gordon, and R. J. Cohen, "An efficient algorithm for spectral analysis of heart rate variability," *IEEE Trans. Biomed. Eng.*, vol. BME-33, pp. 900–904, 1986.
[14] G. B. Moody, "ECG-based indices of physical activity," in *Computers in Cardiology*. Piscataway, NJ: IEEE Computer Society Press, pp. 403–406, 1992.
[15] M. Merri, D. C. Farden, J. G. Mottley, and E. L. Titlebaum, "Sampling frequency of the electrocardiogram for spectral analysis of the heart rate variability," *IEEE Trans. Biomed. Eng.*, vol. 37, no. 12, pp. 99–105, 1990.
[16] P. Castiglioni, "Evaluation of heart rhythm variability by heart or heart period: Differences, pitfalls and help from logarithms," *Med. Biol. Eng. Comput.*, vol. 33, pp. 323–330, 1995.
[17] J. Mateo and P. Laguna, "New heart rate variability time-domain signal construction from the beat occurrence time and the IPFM model," in *Computers in Cardiology*. Piscataway, NJ: IEEE Computer Society Press, p. , 1996, to be published.
[18] P. Albrecht and R. J. Cohen, "Estimation of heart rate power spectrum bands from real world data: Dealing with ectopic beats and noise data," in *Computers in Cardiology*. Piscataway, NJ: IEEE Computer Society Press, pp. 311–314, 1989.

[19] C. L. Birkett, M. G. Kienzle, and G. A. Myers, "Interpolation of ectopics increases low frequency power in heart rate variability spectra," in *Computers in Cardiology*. Piscataway, NJ: IEEE Computer Society Press, pp. 257–259, 1992.
[20] R. L. Burr and M. J. Cowan, "Autoregressive spectral models of heart rate variability," *J. Electrocardiol.*, vol. 25 (Suppl.), pp. 224–233, 1992.
[21] G. Baselli, S. Ceruti, S. Civardi *et al*., "Heart rate variability signal processing: A quantitative approach as an aid to diagnosis in cardiovascular pathologies," *Int. J. Biomed. Comput.*, vol. 20, pp. 51–70, 1987.
[22] D. J. Christini, A. Kulkarni, S. Rao, E. Stuttman, F. M. Bennet, K. Lutchen, J. M. Hausdorff, and N. Oriol, "Uncertainty of AR spectral estimates," in *Computers in Cardiology*. Piscataway, NJ: IEEE Computer Society Press, pp. 451–454, 1993.
[23] G. B. Moody, "Spectral analysis of heart rate without resampling," in *Computers in Cardiology*. Piscataway, NJ: IEEE Computer Society Press, pp. 715–718, 1993.
[24] N. R. Lomb, "Least-squares frequency analysis of unequally spaced data," *Astrophysical and Space Science*, vol. 39, pp. 447–462, 1976.
[25] J. D. Scargle, "Studies in astronomical time series analysis II. Statistical aspects of spectral analysis of unevenly spaced data," *Astrophisical J.*, vol. 263, pp. 835–853, 1982.
[26] A. V. Oppenheim and A. S. Willsky, *Signals and Systems*. Englewood Cliffs, NJ: Prentice-Hall, 1983.
[27] A. V. Oppenheim and R. W. Schafer, *Discrete-Time Signal Processing*. Englewood Cliffs, NJ: Prentice-Hall, 1989.
[28] W. H. Press and G. B. Rybicki, "Fast algorithm for spectral analysis of unevenly sampled data," *Astrophysical J.*, vol. 338, pp. 277–280, 1989.
[29] W. H. Press, S. A. Teukolsky, W. T. Vetterling, and B. P. Flannery, *Numerical Recipes in C: The Art of Scientific Computing*, 2nd ed. Cambridge, U.K.: Cambridge Univ. Press, 1992.
[30] O. Rompelman, J. B. I. M. Snijders, and C. J. van Spronsen, "The measurement of heart rate variability spectra with the help of a personal computer," *IEEE Trans. Biomed. Eng.*, vol. BME-29, pp. 503–510, July 1982.
[31] A. B. Carlson, *Communication Systems, an Introduction to Signal and Noise in Electrical Communication*, 3rd ed. New York: , MacGraw Hill, 1986.
[32] O. Rompelman and H. H. Ros, "Coherent averaging technique: A tutorial review. Pt. 1: Noise reduction and the equivalent filter; Pt. 2: Trigger jitter, overlapping responses and nonperiodic stimulation," *J. Biomed. Eng.*, vol. 8, pp. 24–35, 1986.
[33] J. S. Bendat and A. G. Piersol, *Random Data. Analysis and Measurements Procedures*. New York: Wiley, 1986.
[34] E. J. Bayly, "Spectral analysis of pulse frequency modulation in the nervous systems," *IEEE Trans. Biomed. Eng.*, vol. BME-15, no. 4, pp. 257–265, Oct. 1968.
[35] L. T. Mainardi, A. M. Bianchi, G. Baselli, and S. Cerutti, "Pole-traking algorithms for the extraction of time variant heart rate variability spectral parameters," *IEEE Trans. Biomed. Eng.*, vol. 42, pp. 250–259, 1995.
[36] G. B. Moody and R. G. Mark, "The MIT-BIH arrhythmia database on CD-ROM and software for use with it," in *Computers in Cardiology*. Piscataway, NJ: IEEE Computer Society Press, pp. 185–188, 1990.
[37] A. Taddei, A. Biagini *et al*., "The European ST-T database: Development, distribution and use," in *Computers in Cardiology*. Piscataway, NJ: IEEE Computer Society Press, pp. 177–180, 1991.

Pablo Laguna (M'92) was born in Jaca (Huesca), Spain in 1962. He received the M.S. degree in physics and the Ph.D. degree in physic science from the Science Faculty at the University of Zaragoza, Spain, in 1985 and 1990, respectively. His Ph.D. degree thesis was developed at the Biomedical Engineering Division of the Institute of Cybernetics (U.P.C.–C.S.I.C.), Politecnic University of Catalonia, Spain, under the direction of P. Caminal.

He is an Associated Professor of Signal Processing and Communications in the Department of Electronics Engineering and Communications at the Centro Politécnico Superior, University of Zaragoza. From 1987 to 1992 he worked as Assistant Professor of Automatic Control in the Department of Control Engineering at U.P.C., and as a Researcher at the Biomedical Engineering Division of the Institute of Cibernetics (UPC-C.S.I.C.) His professional research interests are in signal processing, particularly in biomedical applications.

George B. Moody (A'94) was born in 1954 in Nouasseur, Morocco. He studied physics at the Massachusetts Institute of Technology (MIT), Cambridge.

Since 1977, he has been affiliated with the Harvard-MIT Division of Health Sciences and Technology, where his work has included design and development of algorithms for analysis of the ECG and other physiologic signals, and design and development of statistical methods and standard databases of physiologic signals for algorithm testing. He has served on several standards-writing committees of the Association for Advancement of Medical Instrumentation (AAMI) since 1983. His research interests include automated analysis of physiologic signals, statistical pattern recognition, design of physiologic signal databases, heart rate variability, neural networks, and applications of artificial intelligence and advanced digital signal processing techniques to multiparameter physiologic monitoring.

Roger G. Mark (S'59–M'83–SM'95) was born in 1939 in Boston, MA. He received the S.B. and Ph.D. degrees in electrical engineering from Massachusetts Institute of Technology (MIT), Cambridge, in 1960 and 1966, respectively, and the M.D. degree from Harvard Medical School, Cambridge, MA, in 1965.

He trained in internal medicine at Boston City Hospital and served two years in the USAF Medical Corps from 1967–69 studying biological effects of laser radiation. He joined the MIT faculty in electrical engineering in 1969, where he is currently Professor of Electrical Engineering and Computer Science and of Health Sciences and Technology. His research interests are in the areas of physiological signal processing and intelligent patient monitoring.